

Reply to Editor

Thank you again for your interesting submission "Low cost, multiscale and multi-sensor application for flooded areas mapping" as well as for the response to the comments of the referees.

The referees agree that the manuscript is of interest for the readers of NHESS and the flood risk community.

Combining the reports, it appears to be necessary to provide more details about data and data processing steps as well as quantitative information about the performance and accuracy of classifications. Further, the need was stressed to provide a flow chart of the data sources, processing steps and results.

AC: Dear Kai Schröter, We would like to thank you for the reading of the manuscript discussion.

Following the suggestion of the referees we provided to improve the manuscript. In particular, we gave more detail about Como-Skymed and MODIS data processing. We also add more quantitative results in the discussion chapter as required by the referees. We also add a flow chart showing the flood mapping strategy used for this work. (Fig. 13). We also improved figure 4 and figure 9 respect to the first submission.

In addition, I would like to emphasize that you conduct a thorough English proof-reading and check of correct referencing, e.g. Guy et al. ,2015 is actually Schumann et al., 2015. Please also make sure to correctly and consistently reference online sources.

AC: We revised English, using an advanced grammar proofreading software and with a careful re-reading and we corrected the wrong references.

Your responses seem to take-up the constructive comments of the referees and will allow to present your approach and results more clear. Therefore, I decided for minor revision and I will review your revised manuscript.

AC: In this document we provide the response (AC) point-by-point to the referee's comment (RC). The main change to manuscript are reported in *italics* font and also the line and number of the page of the corresponding track change manuscripts are reported (Page X – line XX)

Reply to Referee #1

RC - Reviewer comment; **AC – Authors comment**

The manuscript includes an original study on flood mapping using various remote sensing image sources and techniques. Therefore it has practical significance. In the literature, as also referenced in the study, there are so many research articles studying the evaluated data types and the techniques, however this study uses most of the available data sources and techniques for a single case showing the efficiency of results. Therefore, a comparative study in which the results of maps using optical and SAR images processed with different remote sensing techniques is presented.

In general, the proposed approach was explained well, the experiments were conducted properly, and the results were discussed in the manuscript. However, there still exists some missing points in the manuscript in terms of the completeness of the paper. Therefore, if they are corrected considering the minor issues highlighted below, the article is recommendable for publication.

Reviewer recommends: Minor revision

R: we would like to thank you the Reviewer for the detailed revision and his important suggestions. We improved the manuscript following your input. In the following, we present reviewer's suggestions and relative answers.

In section 3.1.1

RC -1) It is noted that available COSMO-SkyMed image has been classified into three main land cover classes as; water-covered areas, i.e., flooded (low amplitude), urban areas (high amplitude) and soil/vegetation (intermediate amplitude). There, what is the type of the classification method used? The result of the accuracy assessment of the classification process was not given?

AC – 1) thank you for the request. We have improved the manuscript with a more detailed explanation. In particular, we added (Page 7 – line 179): *“The Cosmo-SkyMed image provided is a simple, not-geocoded image in grayscale format (0-255). After the geocoding we re-classify the SAR amplitude images using empirical thresholds in three main classes: water covered areas (0-60) soil/vegetation (60-160) and urban area (160-255). The investigated area is almost flat, so it is not affected by problems related to geometrical distortions. The validation of the data accuracy was made by comparing the reclassified image with aerial photos, optical images, and land-use.”*

RC - 2) Authors are recommended to give at least the overall accuracy of the classification! Please also note that in section 4.1.1, the classification accuracy of COSMO-SkyMed was not presented.

AC – 2) We verified the accuracy in terms of classification reliability of this method using aerial photo and CORINE land-use. We also add the table 6 where is resumed accuracy in terms of flooded area detection. About the section 4.1.1 We modified the text (Page 14 line 389):

I) Co-flood mapping, reclassified amplitude of COSMO-SkyMed data. Results of image classification are shown in Figure 3A, where three classes of SAR amplitude were defined by means of empirical thresholds: i) low that correspond to water covered area (blue); ii) intermediate like soil/vegetation (green); iii) high that are urban areas (pink). In the figure are also overlapped the quarry lake from ancillary data (cyan). The accuracy in the correct detection of land-use type is quite good ranging from 80 % for soil and vegetation, 67% for urban area to 61% for water body (tested in quarry lakes). Vegetation and buildings are factors that reduce the detection of water covered areas even using a full-resolution images and more complex processing (Pierdicca et al., 2018). In a second step we selected with a GIS query the low resolution (water covered) class that mostly correspond to the inundated areas and we compared with the real flooded area. Also the accuracy in the correct detection of flooded areas is quite good: it ranges from 57 % in the lower Oitana stream to 2% in the Po area near Moncalieri. This is related to the time of satellite acquisitions (05:05 UTC of 26 November 2016) some hour before the flood peak. This can be appreciated especially along the Po river, where upstream (near Pancalieri) about the 40% of flooded area was detected, while downstream (Carignano) decrease to 10%. The urban area of Moncalieri limits the capability detection of inundated areas. The false positive errors are less than 5% of the area.

In Section 3.1.2

RC – 3) Did the authors apply atmospheric correction to MODIS data?

AC – 3) this is an important question. In the first version of the manuscript we did not apply atmospheric corrections, but then we searched for already corrected product and we made a comparison with the original dataset. In particular,

we used MYD09 processed images: (Vermote E. - NASA GSFC and MODAPS SIPS - NASA. (2015). MYD09 MODIS/Aqua L2 Surface Reflectance, 5-Min Swath 250m, 500m, and 1km. NASA LP DAAC. <http://doi.org/10.5067/MODIS/MYD09.006>). We compared the corrected images with the previous ones and, since the study area is small and the available atmospheric parameters for correction have 1 km of spatial resolution (water vapour, ozone or aerosol), we did not find significant changes.

We also wrote in the manuscript that no further atmospheric correction was applied to MODIS image.

RC - 4) It was also noted that a supervised classification was applied to MODIS by SAGA-GIS. Which supervised classification method was used? Quantify the accuracy of the classification result.

AC – 4) We used Maximum Likelihood method with absolute probability reference. For this revisions we refined the classification, using corrected images, and we also add spectral angle classification. To answer to the question related to accuracy, in terms of flood detection capacity, please see new table 6. In the manuscript we re-write as follow (page 9 line 237):

Supervised classification of co-flood image. Supervised classifications have already been used in literature to map flooded areas, using machine learning, as described in Ireland et al., (2015). In our work we made a simple supervised classification with SAGA GIS. We first manually defined the training areas with principal land use typologies visible on the false colour image. We try different methodologies for the classifications and we chose as most accurate the maximum likelihood with absolute probability reference and spectral angle methods. We validate the reliability of these classifications with a comparison with false colour image and land-use database. Then we used a GIS query extracted the category “area covered by water or wetland” that mostly correspond to the flooded area for accuracy statics reported in result chapter.

In Section 3.2.1 and 3.2.2

RC - 5) DSM is generated from high resolution images. Digital Surface Model (DSM) is not a Digital Terrain Model (DTM). Authors should know the difference between surface and terrain model.

AC – 5) Yes. We used LIDAR DTM downloaded from Regione Piemonte for our Water Depth models (section 3.3). The Digital Surface Model (DSM) was produced by us from SfM processing of aerial and UAV images and we used DSM for 3D model and for the detection of geomorphological features but as a base layer for WD model. We checked in the manuscript if the terms DTM and DSM were properly used.

In section 3.3

RC – 6) How did the authors perform water level measurements by GPS-RTK positioning? Give a little detail.

AC – 6) We modified the text to fix this issue: we validated and integrated SfM measures of water level using manual measurement of water level geolocated with high precision using a GPS-RTK positioning.

In section 4.1.2

RC – 7) In Figure 4, in the figure caption, the letter of the final item D) appears as C) second time! Correct it:

AC – 7) Ok we corrected it and a new version of figure 4 was made (see below)

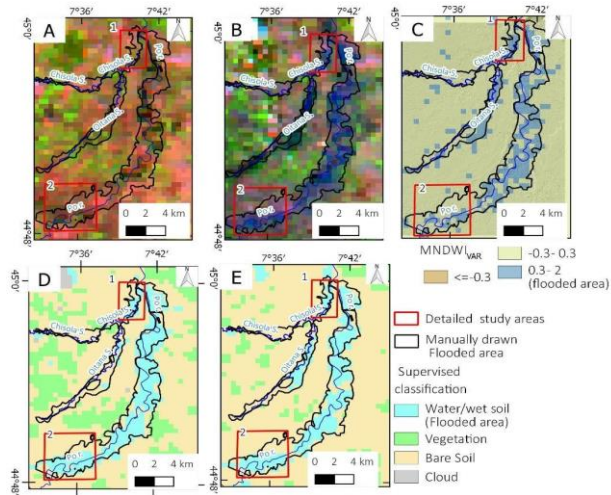


Figure 4: MODIS Aqua satellite image A) False colour band composition 7-2-1 acquired the 12 November 2016.; B) False colour band composition 7-2-1 acquired the 26 November 2016.; C) automatic detection of the flooded area using $MNDWI_{var} > 0.3$; automatic detection of the flooded area using supervised classification with maximum likelihood method (D) and with spectral angle method (E). The red box identifies the local case history of Moncaleri (1) and Pancalieri (2)

RC - 8) It is observed that MODIS image is classified into Cloud, Water, Wet soil, Vegetation, and Bare soil whereas COSMO-SkyMed image has been classified into three main land cover classes as water-covered areas (i.e., flooded), urban areas, and soil/vegetation. It looks like only a GIS query can be done between the classes "Water" and "Water-covered areas" classes derived from CSKM and MODIS images, respectively. Authors need to explain in detail how they used maps generated from the classified images.

AC – 8) Yes, we used a GIS query to selected the flooded pixels, but for each dataset the query is based on different criteria; in particular:

1. In the case of supervised classifications of MODIS data, flooded pixels correspond to water or wet soil classes. We modify the manuscript (Page 15 line 453) as follows:
"Supervised Classification. We also made a supervised classification of 26 November MODIS image using maximum likelihood (MLC) (Fig. 4 D) and spectral angle (SA) (Fig. 4 E) methods. In the study area, we classified, four primary land cover: vegetation, bare soil, cloud, and water body / wet soil that almost identify the flooded sector (the water bodies likes the quarry lakes are too small for MODIS pixel). After a visual checking of the classification reliability, we used a GIS query to select the "water covered and wet areas" classes. The query creates a boolean rasters of flooded

areas. The accuracy of flood map based on supervised classification is good: it identifies most of the flooded areas for Po river (> 70 %) with low false positive pixel (table 6). Worst results for the are flooded by Chiosla and Oitana.

2. In the case of bands ratio (NDVI, MNDWI) made with Sentinel-2 and MODIS DATA, we adopted numerical thresholds empirically based. In the manuscript we write (Page 15 line 417) "In figure 4 C we identified flooded area using a GIS query with the value $MNDWIvar \geq 0.3$. This value is an empirical threshold that selects most of detectable flooded area and minimizes false positive errors." (Page 16 line 438) "For both indexes we used GIS queries with empirical thresholds to extract the flooded area:"
3. In the case of CSKM, we better specified in the text and in figure 3 that SAR Amplitude Image of CSKM was divided into three classes, based on empirical numerical thresholds, that correspond to different land-use: low (water covered area), medium (soil and vegetation) and high (urban areas). We assumed that water covered areas are almost flooded areas. We modify the manuscript (Page 14 line 389) as already reported in reply to the comment (2).

In addition, in the introduction of par 4.1 (Page 13 line 369) we better write how we have generated maps from classified images:

"The flooded area limits were manually extrapolated considering satellite data and geomorphological features obtained using the hillshade model derived from 5-m DTM of Regione Piemonte and used as a benchmark for the evaluation of the performance of remote sensing analyses. For Po and part of Chiosla, the flooded areas were also mapped with the help of water height simulation on the base of DTM."

Is now changed as follow:

"We manually extrapolated the flooded area perimeters considering both satellite data and geomorphological features observed in the hillshade model derived from 5-m DTM of Regione Piemonte. For the evaluation of automatic flooded area maps based on satellite data we applied a GIS query for each map to create boolean rasters of flooded / not flooded area. Then we overlap the raster with manual polygon for a geo-statistical analysis and accuracy evaluation as reported in table 6."

In Section 4.2.3

RC - 9) Authors declared that " During the post-processing, we realized that the quality of the images extracted from the video was insufficient for the SfM application. For this reason, after a month we performed a second survey along the same path" Explain the insufficient qualifications for the extracted images used for the SfM application.

AC – 9) Yes, we add the following sentence: (Page 19 line 532) "...the bitrate was too low and the frames are too pixelated. For this reason, after a month we performed a second survey with a higher bit rate along the same path, but only six marks still visible (Fig 10 A)".

In Section 5

RC - 10) It was written that "....." the combined used of InSAR data of Sentinel-1 and Cosmo, and multispectral data of MODIS-Aqua and Sentinel-2 allowed creating maps of the flooded area. InSAR data showed a good performance in the real-

time flood mapping while are weaker for post-event mapping....." Here, instead of InSAR data the use of SAR data is recommended. It is because, the only amplitude value of the SAR data was used and no interferometric process was applied.

AC – 10) Yes it is true, we have corrected it.

In the discussion and results section

RC - 11) Rather than using expressions such as "good agreement", "more precision", "good accuracy", etc; quantify the accuracy or the quality of maps, results, etc .

AC – 11) Thank you for your suggestion, we add some quantitative evaluation of quality of the maps in this section. At end of section 4.1 we also add the table 6 that quantifies the accuracy in flood detection for the automatic processing that we used

Table 6. Accuracy in automatic flooded and not flooded area detection

| Sector | Area km ² | Sentinel-2 | | MODIS-Aqua | | | CSKM | Sentinel-1 |
|-----------------|-------------------------|----------------------|---------------------|----------------------|-----|-----|-----------|------------------|
| | | MNDWI _{var} | NDVI _{var} | MNDWI _{var} | MLC | SA | Recl Ampl | $\Delta\sigma^o$ |
| Not Flooded | 259.5 | 87% | 87% | 91% | 94% | 95% | 96% | 99% |
| Flooded area | | | | | | | | |
| - Po | 47.8 | 48% | 37% | 49% | 70% | 64% | 23% | 4% |
| - Oitana | 11.6 | 49% | 42% | 60% | 11% | 36% | 37% | 1% |
| - Chisola | 7.3 | 21% | 51% | 30% | 24% | 23% | 12% | 1% |
| - Chisola urban | 1.1 | 4% | 24% | | | | | |

RC - 12) Last but not least, the difficulty of this study is that the satellite data might have not always been received at the time of the hazard occurred! The authors can add a better flow chart that shows the missing data can be replaced by the other, taking into account the image data sorted from high resolution to low resolution:

AC – 12) Yes, it is true: the time of satellite pass over the flooded area is a limit especially with fixed revisit time sensors that we decided to use. Following your suggestion, we create a better flowchart in which we purpose the parameters for the choice the data used for flood mapping.

In the manuscript we add this chart as figure 13 and we add the section 4.3 in which our model is explained (Page 20 line 567):

4.3 A flood mapping strategy flow chart

The flowchart in figure 13 shows the approach that we purpose for the choice of instruments and methods to map the flooded areas, based on the results of this study.

If free satellite data are available, it is possible to sort them taking into account the parameters of time elapsed from flood and the spatial resolution:

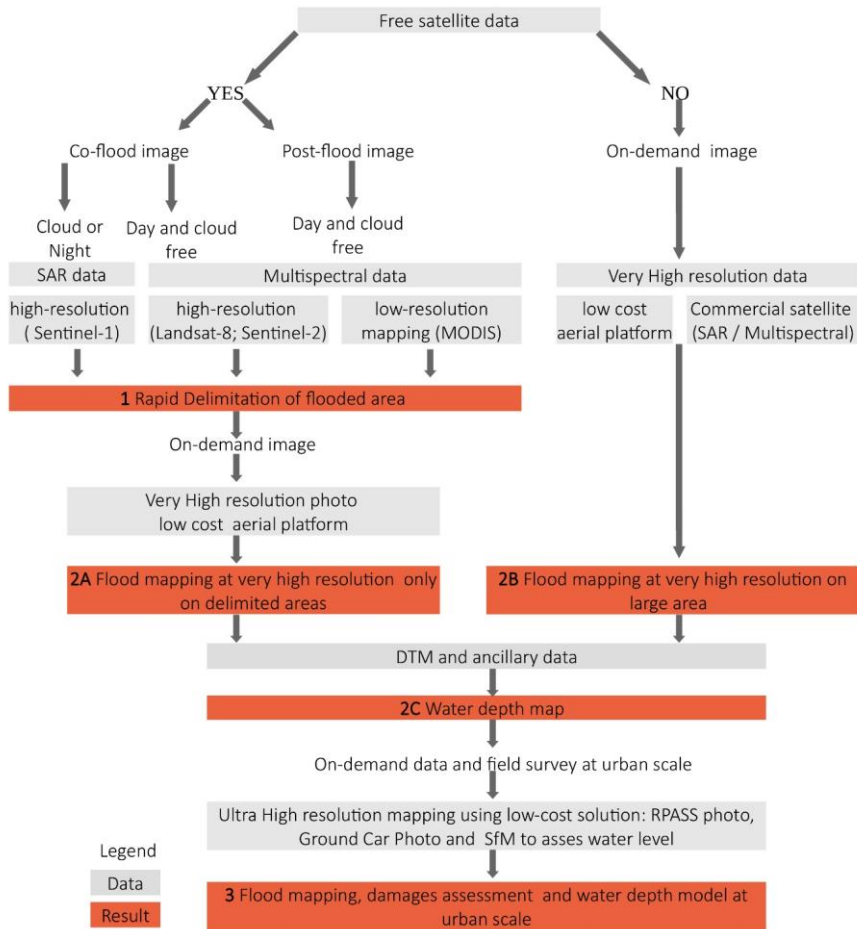
I) The priority is to search for co-flood images that allow an easy mapping. In case of night and cloudy conditions it is necessary to use SAR image (Sentinel-1) while for multispectral data acquired during the day the choice is related to spatial resolution: for instance, Sentinel-2 or Landsat-8 data are more resolute than MODIS data.

II) In the case we have post-flood satellite pass only multispectral data can be used. Also this case the Spatial Resolution and time elapsed from the flood are the parameters that should drive the choice. The use of post-flood data implies more

complicated post-processing (e.g., bands index variation) and with the support of ancillary data to extract the flooded area map. In general, the rapid access to data portal of free satellite data allows to download the data and to make an evaluation of the best solution for the case under study, that not necessarily is the data with high spatial resolution.

After this step it is possible to make a first delimitation of flooded areas, that in case good data may be an already corrected and ready to use map. Then it is possible to focus the acquisition of on-demand of high-resolution sensors only in the most critical or unclear areas (case 2A). If we use only on-demand data, without rapid satellite mapping, we could map at high-resolution large areas (case 2B). This solution however implies higher cost. In case of direct mapping at very-high resolution it is better to use low-cost aerial platforms that are more flexible respect to commercial satellites. After the integration with DEM data the water depth model at basin scale (2C) should be the final result of this chain.

Urban area flood mapping (3) can be considered a hotspot priority inside the general flood map. It needs a more accurate and high-resolution mapping with use of ground-based measures (like SfM model based on car photo), RPASS survey, and the creation of a water depth model that is essential for a precise flood magnitude assessment.



Reply to Referee #2

RC - Reviewer comment; AC – Authors comment

RC - The authors address an interesting and important topic in the field of flood emergency. Several studies are developing methods to integrate remotely-sensed data to produce inundation maps and to estimate hydrological parameters at different time and spatial scale. This study focus on the use of low-cost datasets for this kind of activities, applying different datasets at different scale to derive maps and useful hydraulic parameters as Water Depth and Water Level. My overall opinion about the paper is good and I think is suitable for publication. However, I suggest the authors to point out and better explain some aspects of the analyses.

AC - The authors would like to thanks Domenico Campolongo for his useful revision and suggestions. We reply point-by-point in this document

RC- 1. The use of Cosmo-sky images at full resolution is nowadays also a low-cost option and would provide a definitely more accurate mapping of the inundated areas. Why this option has not been considered instead of the 60 m x 60 m images?

AC -1. Yes, CSK is a low-cost option, especially on the Italian territory, where the acquisition is also more regular and frequent. Our idea, however, was to use as much as possible FREE-COST satellite data with regular acquisition plans on the whole Earth. When we selected the SAR data to be used, we initially focused on the COSMO-SkyMed sensor because, in our example, the time of the satellite acquisitions were optimal to study the wave of flood. However, the analysis of the backscattered signal as seen by a couple of Sentinel-1 images, acquired before and after (two days later) the flood peak, has allowed us to detect and study the modifications of the terrain backscattered signals in a few isolated areas that were inundated after the flooding peak. This analysis was performed by proper radiometric calibration of the SAR images, ending up with maps of the pre-/post-flooding backscattered signal difference at a spatial resolution of about 20 m x 20 m. Even though a simple CSK preview image was used, the capability to detect the flooded areas was fully preserved. This demonstrates that the detection capability of the inundated areas and the water level is not significantly impaired by using a low-resolution (60 m x 60 m) SAR image. Of course, if we had used a full resolution CSK data, the mapping would have been much more precise in terms of spatial resolution, but with relatively few improvements in terms of detection. See for instance the document at the following link http://emergency.copernicus.eu/mapping/system/files/components/EMSR192_07TORINOSOUTH_DELINEATION_OVER_VIEW_v1_100dpi.pdf describing an experiment where a CSKM full resolution image was used to map the flooded area south of Turin.

RC - 2. Please provide more info about the DTM of Regione Piemonte used to calculate WD (for example time of acquisition, errors on z values etc). Furthermore a discussion of uncertainties in WD and WL estimation is needed.

AC -2. The DTM-Lidar was acquired in 2009-2010, the metadata (in Italian) can be found here <http://www.geoportale.piemonte.it/geonetworkrp/srv/ita/metadata.show?id=2552&currTab=rndt>.

The accuracy of elevation ranges from +/-0.3 m to +/- 0.6 m in urban areas. This accuracy is quite good for our model, and no better DTMs on the whole area are freely available. The uncertainties in our model are more complicated to quantitative evaluate because they depend on many factors. The number of ground-based WD measures as well as their reliability and geolocation represent the main limitations. The interpolation to obtain water table raster is also another source of error. For instance, in the case of Moncalieri where we have good and controlled measurement points, the error can be estimated in the range of +/-0.2 m. On the rest of Po valley the error is greater than 0.5 m. To minimize the errors, we have made several interpolations to detect the best water table raster that defines the real flooded area. In the manuscript we have indicated the DTM accuracy and spent a few words on the model uncertainty.

RC -3. In the discussion the authors mention InSAR but they do not perform any InSAR processing. They only mention $\Delta\sigma$ post-pre-flooding as described in the method section. Please explain.

AC -3. We changed the manuscript to explain our results, better. In the discussion section, we have added (Page 22 line 504): *"We compared pre- and post-flood SAR images of Sentinel-1 making SAR backscattering difference of radiometrically calibrated images. For CSK, we reclassified a simple low-resolution image acquired close to co-flood time. The results show that the timely acquisition of satellite data in the case of a flood event is fundamental: in the areas covered by water (like for CSK data) up to 40% of pixels were correctly classified as flooded and it was possible to detect a clear pattern. On the other hand, SAR is weaker for post-event mapping: in our case, the available data acquired two-three days after the flood (Sentinel-1) support the detection of less than 4% of the flooded area."*

RC -4. At line 509 authors say: "InSAR data showed a good performance in the real-time flood mapping while are weaker for post-event mapping." It is not clear what is intended here for "good performance" and how the performance was evaluated. This aspect needs to be discussed in more detail.

AC -4. As presented in the comment to reviewer 1, in the revised version we have added table 6 where some quantitative evaluation regarding flood detection accuracy/performance have been presented and discussed. We evaluated the performance making a ratio between the flooded detected by automatic processing of SAR data and the real flooded area. For instance, CSK detected 23 % (but higher upstream up to 50% detection) of the area flooded by Po, whereas Sentinel-1 reach only 4%. The false positive cases (not flooded area classified as flooded) were also evaluated in the accuracy assessment (SAR data have less than 5 % false positive).

RC -5. In general I think that in the paper some kind of assessment (better if quantitative) of the results is lacking

AC -5 As introduced in the previous comment, we have added table 6 where we reported some quantitative evaluation of satellite data results. In the manuscript, we have also added more details about the validation process of our results. Some other quantitative data about flood extension and water depth model results in the study area have been added to the discussion/conclusion section.

In addition, as suggested by the reviewer 1, we have added a flow chart that shows our approach for mapping flooded areas. This flowchart is based on the results of our study, but we hope that the schema can be considered for a more general approach for low-cost flood mapping

You can find the new flowchart at the following link:

<https://www.nat-hazards-earth-syst-sci-discuss.net/nhess-2017-420/nhess-2017-420-AC1-supplement.pdf>

Reply to Referee #3

RC - Reviewer comment; AC – Authors comment

RC - The authors carried out a comprehensive study on the use and integration of data from multiple sensors for flood mapping. They used some approaches already tested in literature and others more innovative and experimental. In particular, they designed an approach using free or low-cost data/sensors that was tested on a real case study considering both urbanized and not urbanized areas.

The work is certainly of interest for the readers of NHESS. Nevertheless, I have a number of comments that may help the authors in improving the final quality of the manuscript.

AC - The authors would like to thanks Salvatore Manfreda for his useful revision and suggestions. We reply point-by-point in this document.

RC - 1) In order to provide enough information to replicate the experiment, I would suggest to include more details about the methods used for the classification of the satellite images (COSMO-Skymed, Aqua satellite co-flood image).

AC –1. thank you for your suggestion. As also suggested by another reviewer, we improve the description of the type of data and processing used for COSMO-Skymed and MODIS-Aqua satellites. In particular:

a) For Cosmo-data in section 3.1.1 (Page 7 line 179):

“The Cosmo-Skymed data provided is a simple, not-geocoded, image in greyscale format (0-255). After the geocoding, we re-classify, using GIS software, the SAR amplitude images using empirical thresholds in three main classes: water covered areas (0-60) soil/vegetation (60-160) and urban area (160-255). The investigated area is almost flat, so it is not affected by problems related to geometrical distortions. The validation of the classification accuracy was made by comparing the reclassified image with aerial photos, optical images, and land-use.”

b) For MODIS-Aqua: for this the revisions we used the atmospheric calibrated data and we added a sentence to the manuscript (section 3.1.2) (Page 8 line 224):

“For the elaboration, we used the MYD09 - MODIS/Aqua Atmospherically Corrected Surface Reflectance 5-Min L2 Swath 500m, (Vermote, 2015) downloaded from <http://ladsweb.nascom.nasa.gov/>.”

We also better explain how we made the supervised classification with this new paragraph (Page 9 line 237): *“Supervised classification has already been used in literature to map flooded areas, using machine learning, as described in Ireland et al., (2015). In our work we made a simple supervised classification with SAGA GIS. We first manually defined the training areas with main land use typologies visible on the false colour image. We tried different methodologies for the classifications and we chose as most accurate the maximum likelihood with absolute probability reference and spectral angle methods. We validate the reliability of these classifications with a comparison with false colour image and land-use database. Then, using a GIS query, we extracted the category “area covered by water or wetland” that mostly correspond to the flooded area for accuracy statics reported in the result section.”*

RC - 2) It is notable a relevant amount of manual operations, as stated in several sentences: - Section 3.1 Flood mapping at regional scale with satellite data *"For every considered dataset, we produced a map of the flooded area: We use a visual-operator approach to map flooded areas as resulted more precise than automatic classifications especially in the case of post-flood images"*;

3.1.2 Multispectral satellite data, I) Medium-Low resolution satellite data: *"For the identification of flooded areas, we make the following elaborations: a) False colour image made with combinations of 7-2-1 bands for a visual interpretation of flooded areas"*;

3.1.2 Multispectral satellite data, I) Medium-Low resolution satellite data: *"Supervised maximum likelihood classification of co-flood image made with SAGA GIS. We manually defined the training areas with main land use typology visible on the image."*

3.1.2 Multispectral satellite data, II) Medium-high resolution satellite data: *"To detect flooded area, we first made a visual interpretation using images (Sentinel-2 images) with different bands composition of post-flood data."*

3.2.3 Ground-based ultra-high resolution images: *"For the identification and mapping of water levels, the video is analysed and a frame sequence is extracted from it when the operator sees some marks lefts by water over facades."*

4 Results, Flood mapping from low to medium-high resolutions with satellite data: *"The flooded area limits were manually extrapolated considering satellite data and geomorphological features obtained using the hillshade model derived from 5-m DTM..."*

4.1.2 Flood mapping with multispectral data, I) Multispectral low resolution, MODIS-Aqua: *"MNDWI variation (MNDWIVAR) at 20 m of spatial resolution: However, like for NDVI, the presence of many areas with positive variations outside the flooded sector makes more accurate a manual interpretation."*

4.1.2 Flood mapping with multispectral data, II) Multispectral medium-high resolution post-flood mapping Sentinel-2: *"The images of Sentinel-2 were analysed by visual interpretation of RGB composite image and using two different indexes (NDVI - MNDVI) to identify flooded areas shown in figure 5."*

Therefore, I am wondering if such an approach might still be considered low-cost and fast, considering the amount of work that needs to be performed by human operators. Also, the reliability and accuracy of the results would significantly depend on the ability and experience of the operator.

AC -2. Thank you for your suggestions. In the following our reply:

a) About the cost: We considered this approach low-cost because we used only free satellite data for regional mapping. With actual revisit frequency of free sensors in most of the events, it should be possible to avoid or limit the on-demand commercial satellite or traditional aerial flight over a large area that have high costs and not always can be planned.

For instance, for Piemonte flood the cost of traditional aerial survey was about 80'000 € (about 130 €/km²) http://www.regione.piemonte.it/governo/bollettino/abbonati/2017/28/attach/dda180000620_660.pdf (Regione Piemonte, 2017 Italian)

Where is necessary to have a high-resolution mapping, we proposed low-cost (respect to traditional methods) sensors. Go-pro cameras or the RPASs now have affordable costs. Also the aerial photos that we used have a low cost compared to the traditional aerial platform.

b) About the rapidity in flood mapping: We agree that our manual approach cannot be fast as an automatic classification mapping like the EMSR service, but our aim is different from providing an early warning /emergency mapping that is not validated and represents the inundated area at a specific instant.

Our method has the aim to provide (low cost) maps of the flooded area and water depth with good accuracy and with a reliable validation. These maps, like the maps provided by official authority (e.g., ARPA Piemonte in our case) could be used for a post-flood damages assessment or to improve urban planning and to evaluate damages.

Free satellite images are available few hours or at least one day after their acquisition. Moreover, it is possible to know in advance the time of satellite pass. The processing both for SAR and multispectral satellite data could be made in few days like the water depth model based on DEM.

It is possible to estimate that within few weeks after the flood to have a good map of the flooded area.

At local scale, RPAS, aerial photo and Car Camera surveys can be made in few days, while post-processing and SfM elaboration and data validation require few weeks of work.

c) About human operator: the human factor (operator ability) is crucial, but our method is proposed for people who have expertise in flood mapping (e.g., geomorphologists or remote sensing operator who work in regional services, academia). Moreover, our methods are mostly based on simple raster GIS calculations that can be easily replicated.

The automatic detection of flooded area works only if we have perfect co-flood image, otherwise an interpretation is necessary. This analysis takes into account also local conditions (geomorphology of flooded are, anthropic structure).

RC - 3) It is not possible to infer the performances of the methods/data investigated. Please, describe and provide results of any statistical analyses that you performed:

AC -3. We thank for your suggestion. In the answer to reviewer 1 we presented a new table (Table 6) in which we show the performances of data and methods that we used.

| Sector | Area km ² | Sentinel-2 | | MODIS-Aqua | | | CSKM | Sentinel-1 |
|-----------------|-------------------------|----------------------|---------------------|----------------------|-----|-----|-----------|------------------------|
| | | MNDWI _{var} | NDVI _{var} | MNDWI _{var} | MLC | SA | Recl Ampl | $\Delta\sigma^{\circ}$ |
| Not Flooded | 259.5 | 87% | 87% | 91% | 94% | 95% | 96% | 99% |
| Flooded area | | | | | | | | |
| - Po | 47.8 | 48% | 37% | 49% | 70% | 64% | 23% | 4% |
| - Oitana | 11.6 | 49% | 42% | 60% | 11% | 36% | 37% | 1% |
| - Chisola | 7.3 | 21% | 51% | 30% | 24% | 23% | 12% | 1% |
| - Chisola urban | 1.1 | 4% | 24% | | | | | |

In the manuscript we explain how we evaluated the performance (introduction of chapter 4 paragraph (Page 14 line 371):
“For the evaluation of automatic flooded area maps based on satellite data, we applied a GIS query for each map to create boolean rasters of flooded / not flooded area. Then we overlapped the obtained raster with manual polygons for a geo-statistical analysis, for each polygon is reported the percentage pixel classified as flooded/not-flooded. The main results are reported in table 6.”

We also added more quantitative results in section 5 (discussion / Conclusions):

About SAR (Page 22 line 504)

“Concerning SAR data, we reclassified a simple preview low-resolution Cosmo-Skymed amplitude image acquired some hours before the co-flood time. The results show that the time of satellite pass is fundamental: if the area is covered by water (like upstream part of Po river) up to 60% of pixels was correctly classified as flooded and it was possible to observe a clear pattern. We compared pre- and post-flood SAR images of Sentinel-1 making SAR backscattering difference of radiometrically calibrated images. The result shows that SAR is weaker for post-event mapping: in our case 3 days after the flood (Sentinel-1) less than 4% of the flooded area is still detectable”

About multispectral data (Page 22 line 515)

“The low-resolution MODIS image acquired near the co-flood stage allowed a good identification of flooded areas using different methods: MNDWI variation and supervised classifications. The detection accuracy is good especially for the area flood by Po river where about the 70% of the flooded area was correctly identified.

Medium-High resolution multi-spectral data have more capability with post-event mapping. In this work, we tested NDVI and MNDWI variations for the detection of flooded areas based on the comparison of pre- and post- event images. Both methodologies show quite good performance in cultivated land, (40 % - 45% of accuracy). Here it is possible to detect a clear pattern: inside the inundated area the percentage of pixel classified as flooded is four times greater than in not flooded area. The inundated areas are more difficult to detect in the dense urban area of Moncalieri (only 4% area was correctly mapped).

RC - 4) Probably, after 8 pages of Materials and Methods and 7 pages of Results, the article would benefit from an expanded discussion, where those data are interpreted. I would try to address the following questions: What is the overall advice (if exists) authors can give to readers for an efficient approach for flood inundation mapping? Since appears that some analyses provided results not accurate or too uncertain or under/overestimation too significant, is any of the tested methods and data less relevant than others? Can any of these methods/data be completely replaced by the information provided (with a higher accuracy) by other analysed methods/data?

AC -4. Thank you for your suggestions. We added a flowchart (figure 13), and a paragraph (4.3) in the manuscript to clarify all these points:

1) The most important thing that we would give to readers is that it is not possible to select a priori which type of data/processing is the better for flood mapping. This depends on different factors:

- 1. Time of satellite acquisition respect to the time of flood peak.**
- 2. Type of satellite data (SAR / multispectral, spatial resolution)**
- 3. Study area features and risk (dimension, cloud cover, land-use and element at risk)**
- 4. Affordable cost (e.g., we use commercial satellite data or traditional aerial photo only if they give significant advantages to flood mapping)**

Another aspect is the data policy. The applied use of free data could encourage the authorities (e.g., The European Union) to make further investment in open data.

2) To compare the performance of data and methods would be necessary that all satellites acquired at the same time and this is a rare combination.

For instance, in some cases, a 500 m spatial resolution multispectral image acquired at flood peak could be more accurate than a SAR image with 1 m resolution acquired 2 days after the flood. On the other hand on particular area image from a commercial satellite could be the only one that covers the flood peak. In our case Sentinel-1 show low performance the

Cosmo not for the data quality (Sentinel-1 at full resolution is far better than a quicklook image) but only for the time of satellite pass.

The results of band indexes variation of Sentinel-2 show little better performance of MNDWI respect to NDVI. In urban areas both NDVI and MNDWI performance are very weak (we add this consideration to manuscript)

In the manuscript we added a new paragraph 4.3 (Page 20 line 567):

"4.3 Flood mapping strategy flowchart

The flowchart in figure 13 shows the approach that we purpose for the choice of instruments and methods to map the flooded areas, based on the results of this study. If free satellite data are available, it is possible to sort them taking into account the parameters of time elapsed from flood and the spatial resolution:

I) The priority is to search for co-flood images that allow an easy mapping. In case of night and cloudy conditions it is necessary to use SAR image (Sentinel-1) while for multispectral data acquired during the day the choice is related to spatial resolution: for instance, Sentinel-2 or Landsat-8 data are more resolute than MODIS data.

II) In the case we have post-flood satellite pass only multispectral data can be used. Also for post-flood data, the spatial resolution and time elapsed from the flood are the parameters that should drive the choice. The use of post-flood data implies more complicated post-processing (e.g., bands index variation) and with the support of ancillary data and DTM to extract the flooded area map. In general, the rapid access to data portal of free satellite data allows to download the data and to make an evaluation of the best solution for the case under study, that not necessarily is the data with high spatial resolution.

After this step, it is possible to make a first delimitation of flooded areas, that in case good data may be an already corrected and ready to use map. Then it is possible to focus the acquisition of on-demand of high-resolution sensors only in the most critical or unclear areas (case 2A). If we use only on-demand data, without rapid satellite mapping, we could map large area at high spatial resolution (case 2B). This solution, however, implies a higher cost. In case of direct mapping at very-high resolution, it is better to use low-cost aerial platforms that are more flexible respect to on-demand commercial satellites. The integration with DEM data allows creating the water depth model at basin scale and a further refinement of flooded area maps (2C).

Urban area flood mapping (3) can be considered a hotspot priority inside the general flood map. It needs a more accurate and high-resolution mapping with use of ground-based measures (like SfM model based on car photo), RPAS survey, and the creation of a water depth model that is essential for a precise flood magnitude assessment.

It is important to remind that is not possible to select a priori which type of data/processing is the better for flood mapping. The best method to use depends on different factors: 1. Satellite acquisition and time elapsed from flood peak; 2. Type of satellite data (SAR / multispectral, spatial resolution); 3. Study area features and risk (dimension, cloud cover, land-use and element at risk); 4. Affordable cost (e.g., we use commercial satellite data or traditional aerial photo only if they give significant advantages to flood mapping)"

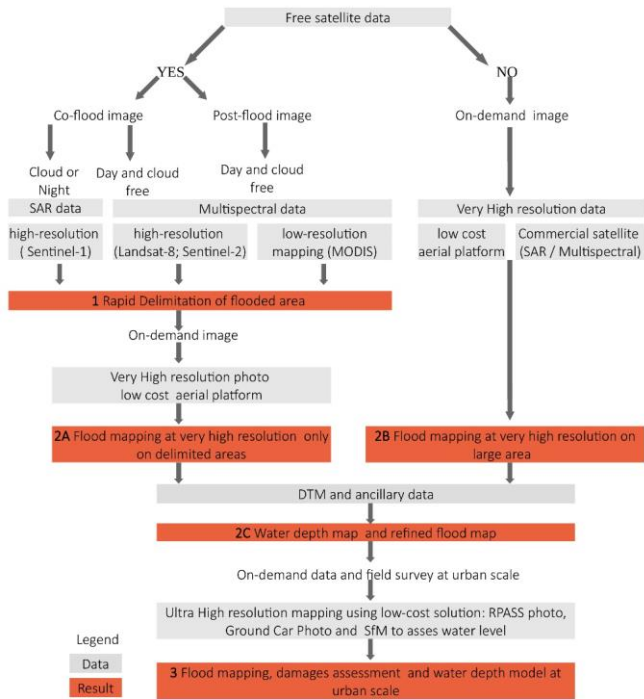


Figure 13: Flowchart of the proposed flood mapping strategy

RC - 5. Minor comments The paper contains a number of typing errors that requires a careful review of the English. Below some examples that I found while reading the manuscript.

AC – 5. Meanwhile the paper was under revision we provided to improve formation and to revise English.

RC – 6. Check the way citations are written in the manuscript. Sometimes "et al" is followed by no full stop and just the comma (Luino et al, 2009) sometimes a semicolon (Wang et al; 2012), sometimes nothing (Boni et al 2016). Other examples in lines 37-38 "Boni et al 2016; Mason et al 2014; Guy et al 2015; Refice et al 2014; Pulvirenti et al; 2011; Clement et al, 2017; Brivio et al; 2002".

AC - 6 - We corrected all the reference using the NHESS format "et al.," Also in the reference section, we have checked for a correct alphabetical index and NHESS format.

RC 8 - Line 42: correct "authorirhyes"

AC 8 – corrected

RC 9 - Line 44: it should be "details" (plural) instead of "detail"

AC 9 - corrected

RC 10 - Lines 47-48: check subject-verb agreement "A partial solution could be the use of a Remotely Piloted Aerial System (RPAS), that are usually able". A RPAS system is singular.

AC 10 - corrected in "Remotely Piloted Aerial Systems"

RC 11 - Line 81: check subject-verb agreement "The basin of Po and Tanaro rivers were"

AC 11 - corrected in basins

RC 12 - Line 90: check subject-verb agreement "the actual plain (Fig. 1 B and Fig 1 C) correspond to"

AC 12– we changed in "corresponds"

RC 13- Line 92: check english "The plain is marked by the terraces that delimit of actual Po valley..."

AC 13 - we changed in (Page 4 line 95): "The fluvial terraces delimit of actual Po valley..."

RC 14 - Lines 122: "pre-flood', 'co-flood' and 'pre/post-flood' data". I suggest you to remove pre-flood and just leave "co-flood' and 'pre/post-flood' data", since in the following lines you distinguish and explain these two categories.

AC 14 - Done

RC 15 - Lines 125-127: "Using a multi-scale approach, we developed a methodology that considers the progressive use satellites and then high and ultra-high resolution systems for the acquisition of a dataset that can be used to support the identification of water level reached by the flood and occurred damages". I think an "of" is missing before "satellites".

I also suggest authors to think about rephrasing or splitting this sentence in two.

AC 15 - now is re-write as follows (Page 5 line 130): "Using a multi-scale approach, we developed a methodology (Fig. 2) that progressively considers the use satellites and then high and ultra-high resolution systems. The aim is the acquisition of a dataset that can be used to support the identification of water depth and extension reached by the flood. The dataset also allowed making a first evaluation of damages both in urbanized and not urbanized areas."

RC 16 - Line 130: "quikly indication". Proper spelling is quickly. By the way, I think the adject-ive form "quick" is the appropriate one.

AC 16- we change quick in general

RC 17 - Line 134 and 137: "Orthophoto" instead of "ortophoto".

AC 17 - done

RC 18 - Line 264: "the system can flight on demand during the flood of immediately after". "Or" instead of "of"
AC 18 - done

RC 19 - Line 332: "to assess" instead of "to assesses"
AC 19- done

RC 20 - Line 363: "The MODIS-Aqua satellite takes an image,, during the late morning of November 26, 2016. " "Took", instead of "takes".
AC 20- done

RC 21 - Line 426: "mapped" instead of "mapp7ed"
AC 21 – done

Low cost, multiscale and multi-sensor application for flooded areas mapping.

Daniele Giordan¹, Davide Notti¹, Alfredo Villa², Francesco Zucca³, Fabiana Calò⁴, Antonio Pepe⁴, Furio Dutto⁵, Paolo Pari⁶, Marco Baldo¹, Paolo Allasia¹

¹National Research Council of Italy, Research Institute for Geo-Hydrological Protection (CNR-IRPI), Strada delle Cacce 73, Torino 10135, Italy;

²ALTEC S.p.A., Torino, 10146, Italy;

³Department of Earth and Environmental Science, University of Pavia, Via Ferrata 1, 27100 Pavia, Italy

⁴National Research Council of Italy, Institute for the Electromagnetic Sensing of the Environment (CNR-IREA), Via Diocleziano 328, Napoli 80124, Italy;

⁵Civil protection Service of Torino, Grugliasco, 10095, Italy;

⁶Digisky S.r.l., Torino, 10146, Italy.

Correspondence to: Davide Notti (davide.notti@irpi.cnr.it)

Abstract

Flooded areas mapping and estimation of maximum water height/depth are important/essential elements for a first damages evaluation, civil protection interventions planning and detection of areas where remedial are more needed.

In this work, we present and discuss a methodology for mapping and quantifying flood severity over plain areas is presented and discussed. The proposed methodology considers a multiscale and multi-sensor approach using free or low-cost data/sensors. We applied this method to November 2016 Piemonte (NW Italy) flood. We first mapped flooded areas at basin scale using free satellite data from low to medium-high resolution using both SAR (Sentinel-1, Cosmo-SkyMed) and multispectral sensors (MODIS, Sentinel-2). Using very- and ultra- high-resolution images from the low-cost aerial platform and Remotely Piloted Aerial System, we refined the flooded area/zone, and we detected the most damaged sector. The presented method considers both urbanized and not urbanized areas. Nadir images have several limitations in particular in urbanized areas, where the use of terrestrial images solved this limitation. Very- and ultra-high resolution images have been processed with Structure from Motion (SfM) for the realization of 3-D models. These data, combined with available digital elevation model, allowed us to obtain maps of flooded area, maximum water high and damaged infrastructures.

1 Introduction

Floods are among the natural disasters that cause major/significant damages and casualties/casualties (Barredo, 2007).

Mapping and modelling areas affected by floods is a crucial task in order to: i) identify the most critical areas for civil protection actions ii) evaluate damages, iii) and make/do correct urban planning. (Amadio et al., 2016). In order to make a precise quantification of damages, a detailed mapping of flooded areas is required, with a good/reasonable estimation of water level

Formattato: Inglese (Regno Unito)

and flow velocity (Arrighi et al., 2013; Luino et al., 2009; Merz, et al., 2010; Kreibich, 2009). Advances in remote sensing and ~~geotechnology~~ technology have introduced the possibility, in last years, of having rapid maps and models during or little time after a flood event (e.g., Copernicus Emergency Management Service (© European Union, 2012-2017)). With satellite remote sensing data, it is possible to map flood effects over ~~widevast~~ areas at different spatial and temporal resolution using multispectral (Brakenridge, et al., 2006; Gianinetto et al., 2006; Nigro et al., 2014; Wang et al., 2012; Yan et al., 2015; Rahman and Di, 2017) or Synthetic Aperture Radar (SAR) images (Boni et al., 2016; Mason et al., 2014; ~~GuySchumann~~ et al., 2015; Refice et al., 2014; Pulvirenti et al., 2011; Clement et al., 2017; Brivio et al., 2002). A good description of main methodologies used to map flood with satellite data has been published by Fayne et al. (2017). ~~In addition~~ Moreover, the increasing availability of free-of-charge satellite data with global coverage (e.g., Sentinel-1 and -2 from ESA, Landsat and MODIS satellites from NASA) makes possible analyses of flooded areas with low-cost solutions. Flood mapping and damages assessment is also an important issue for European Communities ~~authorities~~ authorities that support projects like the Copernicus Emergency Management Service mapping (EMSR) and the European Flood Awareness System (EFAS), which manage the activation procedure to acquire satellite data over the areas affected by a natural hazard. ~~Further detail~~ De Moel et al. (2009) and Paprotny et al. (2017) described further details about different experiences in flood mapping in Europe ~~are described in De Moel et al. (2009) and Paprotny et al. (2017).~~

In urban areas, remote sensing data are often less efficient in the detection of flooded areas, especially if images acquired during the maximum of inundation are not available. A partial solution could be the use of a Remotely Piloted Aerial ~~System~~ Systems (RPAS) (Perks et al., 2016; Feng et al., 2015), that are usually able to acquire ultra-high resolution images over small areas. The quantification of the maximum water level caused by the inundation is ~~an important~~ a crucial parameter in particular in urban areas because it can supply the damages estimations and support civil protection operations (Luino et al., 2009; Bignami et al., 2017). Very often, nadir remote sensed platforms cannot be able to the definition of the level of water and, for this reason, field surveys and ground-based photos are still necessary. A possible solution is the use of models for the estimation of water depth based on DTM or hydraulic model (Bates and De Roo, 2000; Segura-Beltrán et al., 2016), but ground truth validation is needed. Recent developments of computer vision applications like Structure from Motion (SfM) (Snavely, 2008) made this system a possible valid alternative for the ~~acquisition~~ creation of a 3D dataset ~~that based on~~ terrestrial or aerial image acquisition systems. ~~These datasets~~ can be useful for the definition of the level of water depth of flooded areas ~~using terrestrial or aerial image acquisition systems.~~ 3-D models derived from SfM are nowadays used for geomorphological applications (Westoby et al., 2012) and ~~for~~ flood mapping. This second application is often assisted using precise DTM derived from Lidar (Smith et al., 2014; Meesuk et al., 2015, Costabile et al., 2015). Particular applications of SfM can be used to make 3-D models of façades and acquire a ~~useful~~ dataset ~~useful~~ for the identification of marks left by

water. The ~~use of~~ combined use of low-cost systems able to acquire nadiral images and oblique terrestrial ~~oblique~~ pictures is important for the acquisition of a dataset that can be used essential for the definition of water level and the estimation of damages ~~of flooded areas~~ especially for the flooded area in an urban environment (Griesbaum et al., 2017).

65 Finally, geolocated photos or information deriving from the internet and social media (Rosser et al., 2017; Fohringer et al., 2015) or by a volunteer geographic information (Hung et al., 2016, Schnebele and Cervone, 2013) can be ~~very useful~~ handy for improving the mapping of flooded areas.

In this work, we present a smart multi-scale and multi-platform methodology developed for the identification and mapping of flooded areas. The methodology has been tested in two areas struck by the flood occurred in Piemonte (NW Italy) in November
70 2016. The paper presents different case studies that are representative of urban and or not urbanized areas.

2 Study areas

The Piemonte region is located in NW Italy, and most of the territory is inside Po river drainage basin. (Fig 1 A). The Alps range surrounds the region from North to South-Westwest with an elevation higher than 4000 m asl. In the southern sector, Ligurian Alps and Apennines range present lower elevation (1000-2000 m asl) and separate Piemonte from the Liguria sea. At
75 EastOn the eastern side, the basin is open to Po river plain. This orographic setting tends to amplify effects of some particular meteorological conditions like ~~strong~~severe and slow-moving cyclones located at west of Italy that cause a wet flow from South / East that is blocked by Alps range. This meteorological configuration causes heavy rainfalls especially in autumn when the warm Ligurian sea is a source of additional energy and humidity (Buzzi et al., 1998; Pinto et al., 2013). In the last 30 years, ~~4 strong major~~four main floods hit this region: September 1993 (Regione Piemonte, 1996.), November 1994 (Luino, 1999),
80 October 2000 (Cassardo et al., 2013) and November 2016 (ARPA Piemonte, 2016)

In November 2016, a severe flood hit the Piemonte region (NW of Italy). In several areas of Piemonte, in the period 21 – 25 November 2016 different rain gauges registered an amount of rainfall up to 600 mm that represents the 50 % of the ~~main~~mean annual precipitation (Fig. 1 B). The ~~basin~~basins of Po and Tanaro rivers were the most affected by the flood that was very similar, ~~in terms of~~for rainfall distribution and river discharge, to 1994 event, which is considered one of the most destructive
85 occurred in last decades (Luino, 1999). This time, the event caused huge damages, activated numbers of landslides and debris flows and caused the inundation of large areas. The civil protection system managed the emergency, and the number of victims was ~~strongly~~sharply reduced ~~with respect~~compared to 1994 event that caused 70 victims. The 2016 flood caused a victim in Chisone valley, not far from Torino.

90 The presented case study area is located in the Po plain south of Turin city (Fig. 1 C). This area is mainly occupied by intensive agricultural activity and urban areas ~~especially~~ mainly located in the northern part. ~~In At the southern, close to Torino~~ south of Turin, many industrial and commercial areas were built in last decades nearby rivers. From the geomorphological point of view, the actual plain (Fig. 1 B and Fig 1 C) ~~correspond~~ corresponds to the fill of Plio-Pleistocenic Savigliano basin (S.B.), delimited by western Alps, Turin C) Hills (T.H.) and Poirino Plateau (P.P). ~~To west~~ In the western part, it is possible to find alluvial fans of Chisone, Pellice and Chisola streams (Carraro et al., 1995). The ~~plain is marked by the fluvial~~ terraces that delimit of actual Po valley with evident relict geomorphology like paleo-meander. The anthropic influence is remarkable with like quarry lake, revetments and embankment that constrain riverbeds (Fig. 1C). The geomorphology is a keycrucial factor that ~~derived~~ constrains flooded area shape and the water height.

95 This area was affected by the flooded of Po River and other tributaries, in particular, Chisola and Oitana streams causing several damages. The Po river between Carignano and Turin stations reached a maximum discharge of 2000-2200 m³/s in the late evening of 25 November 2016. The main water ~~mean~~ discharge of this monitoring station in November is 70 m³/s. The Chisola stream registered a discharge of 200 m³/s (November average 17 m³/s) near Moncalieri in the afternoon of 25 November (ARPA Piemonte, 2016).

100 Inside this area (Fig. 1 C) we focused our attention in particular on two sites where high-resolution data were acquired:

- 105 • The village of Pancalieri, located in on the left side of Po river, just after the confluence with Pellice river. In this area it is evident the presence of ancient Po river meanders ~~of Po river that~~ which were reactivated by the flood with damages to some settlements and destruction of communications roads.
- The town Moncalieri (about 60'000 inhabitants) is located south of Turin in a ~~very manmade~~ human-made environment. This area was flooded by Chisola stream on the late morning of 25 November partly due to the collapse of some sections of river embankment. The water interested many residential, service and industrial areas with a maximum water ~~heigh~~ height of 1.5 – 2 m. ~~Part~~ Another sector of ~~the~~ Moncalieri municipality was also flooded by Po River in the evening of 25 November, with other damages to commercial and industrial infrastructures.

110 The activation of Copernicus Emergency Management Service (© 2016 European Union) EMSR-192 (<http://emergency.copernicus.eu/mapping/list-of-components/EMSR192>) allowed to map flooded areas (delineation maps) using Radarsat-2, Cosmo-Skymed and Pleiades images in the most critical areas of Piemonte ~~and in~~. In some areas like Moncalieri also a map of damages (grading maps) ~~were~~ was produced. However, the available delineations maps ~~available~~ represent the automatic extraction of the flooded area at the moment of image acquisition, and generally not at the maximum extension. In the case of Piemonte, they cannot be used for exhaustive modelling and damages evaluations. The preliminary ~~estimation~~ estimate of damages to buildings made by the municipality of Moncalieri is about 50 million of € (M€) for industrial

buildings and 13 M€ for residential buildings and others 6 M€ for damages to other goods
120 (<http://www.comune.moncalieri.to.it/flex/cm/pages/ServeBLOB.php/L/IT/IDPagina/3669>).

3 Materials and Methods

The aim of this study is the definition of a possible methodology for the identification and mapping of flooded areas using low
125 ~~cost~~ solutions. For this reason, we have combined and compared data from different sensors, ~~and we~~ We used different
approaches for flood mapping some already tested in literature from long time and others more innovative and experimental.
We first introduce the concept of 'pre-flood', 'co-flood' and 'pre/post-flood' data. Co-flood data are collected around the time
of maximum inundation while pre/post-flood data are acquired before or after the flood maximum. In the first case, the mapping
of flooded areas is ~~obviously easier~~ more straightforward, but the acquisition of co-flood images could not ~~be~~ always be
possible.

130 ~~Our study considers both urbanized and not urbanized areas.~~ Using a multi-scale approach, we developed a methodology (Fig.
2) that progressively considers the progressive use satellites and then high and ultra-high resolution systems ~~for~~. The aim is
the acquisition of a dataset that can be used to support the identification of water level depth and extension reached by the flood
~~and occurred~~. The dataset also allowed making a first evaluation of damages, both in urbanized and not urbanized areas

135 The first identification of the flooded area can be ~~done~~ made using satellites results and in situ information coming from the
civil protection system that collects reports from local authorities (co-flood phase). This first identification phase is mandatory
to have a quickly general and fast indication of the involved area and to plan more detailed acquisitions.

The second phase is aimed to acquire a high definition dataset that can be used for a detailed mapping of the flooded area. For
this step is required a system able to fly on demand over large areas and acquire aan RGB /multispectral dataset with a
resolution of 10-20 cm/pixel. The high-resolution map obtained during this phase can be used for the identification and map
140 of flooded areas with a good acceptable detail. The resolution of the ~~ortho~~ photo ~~ortho~~ photo can also support the identification of
critical elements like damaged infrastructures: bridges, levees, streets and urban areas involved in the flood. The map of most
damaged sectors can be obtained merging civil defence reports and the analysis of acquired ~~ortho~~ photo ~~ortho~~ photos. The
identification of most critical sectors is important essential for a preliminary evaluation of occurred damages and ~~for~~ the
emergency planning of first remedial actions.

145 On the most critical sectors, especially in urban areas, it is possible to acquire ultra-high resolution dataset (2-5 cm/pixel) that
can be used for the quantification of damages or ~~for~~ detailed mapping of flood markers. This third phase can be done using

Remotely Piloted Aerial Systems (RPAS) or terrestrial systems. This last phase is aimed to quantify the flood severity. In our test, we started from the use of nadir images acquired by ~~airplanes~~airplane and RPAS, but we immediately realized that in urban areas this approach ~~can~~could be not sufficient for the mapping of flooded limits and the identification of damages. One of the most ~~important~~critical data is the water level reached by the flood that is often visible only on façades of buildings. The identification and mapping of water level markers on façades are mandatory for a correct reconstruction of what happened. To obtain a 3D representation of urbanized flooded areas, we decided to integrate terrestrial and aerial images using SfM algorithm.

In the following chapters, we present the acquired datasets of different phases (Table 1). All the proposed systems are low-cost solutions that could be adopted by national/regional Authorities with limited efforts.

3.1 Flood mapping at regional scale with satellite data

The developed methodology is based on a multi-scale approach that starts from the use of low-resolution regional scale satellite images. The use of different available satellites images can support the identification of flood effects at low resolution over large areas and at higher resolution at local scale. The choice of the most appropriate satellite data depends on different factors: i) characteristics of the study area, ii) spatial resolution, iii) revisit time, iv) time of acquisitions respect to the moment of maximum inundation, v) availability and cost of images.

In this paper, ~~we considered~~only free of charge images ~~were used~~ to assure a low-cost approach. For every considered dataset, we produced a map of the flooded area that represents the synthesis of remote sensing data and geomorphological evidence from 5-m DTM available from Regione Piemonte. We use a visual-operator approach to map flooded areas as resulted more precise than automatic classifications especially in the case of post-flood images. In table 2 are reported the satellite data ~~in relation~~related to the flood phase. We considered as co-flood data all the images acquired between early November 25 (start of the first inundation) and the evening of November 26, 2016 (withdrawn of water).

3.1.1 SAR data

SAR instruments work in all-weather conditions and in ~~the~~night time, thus ensuring a high observation frequency and increasing the opportunity to provide data in correspondence at the flood event.

I) Co-Flood mapping. If data are available during the maximum flooding phase, it is possible to accurately map the affected area using high-resolution SAR images as those acquired by the TerraSAR-X (Giustarini et al., 2013) and COSMO-SkyMed (Refice et al., 2014) satellites. In particular, the identification of the flooded area is performed by analysing the SAR

175 backscattering, which generally shows low values in water-covered areas. In our analysis, we used a SAR image acquired by the X-band COSMO-SkyMed satellites constellation (wavelength ~ 3 cm) on 25 November (05:05 UTC acquisition time). Data has been provided free-of-charge by E-Geos and Italian Space Agency (ASI) in a quick-look preview format with a 60 m x 60 m resolution.

180 The EMSR service used also Radarsat 2 Cosmo-SkyMed data provided is a simple not-geocoded image in grey-scale format (0-255). After the geocoding, we re-classify through GIS software, the SAR amplitude images for flood mapping. The available COSMO SkyMed image has been classified into using empirical thresholds in three main land cover classes: water-covered areas, i.e., flooded (low amplitude), urban areas (high amplitude) and (0-60) soil/vegetation (intermediate amplitude) 60-160) and urban area (160-255). The investigated area is almost flat, so it is not affected by problems related to geometrical distortions of backscattering. The validation of the classification accuracy was made by comparing the reclassified image with an aerial photo, optical images, and land-use database. The analysis with such data points out the relevance of co-flood images for a fast mapping of flooded areas. We remark that it is not possible to know a priori if a co-flood image will be available during the maximum of the flood event, however, However, the short revisit times achieved by the new generation of SAR satellites can significantly increase the possibility to collect co-flood data.

185 **II) Post-flood mapping.** We also performed a post-flood mapping by exploiting data acquired by the Sentinel-1 mission which is composed of a constellation of two satellites, Sentinel-1A and Sentinel-1B, launched on 2014 April 3, and 2016 April 25, respectively. Sentinel-1A satellites have been designed to acquire C-band SAR data in continuity with the first-generation ERS-1/ERS-2 and ENVISAT mission, developed within the European environmental monitoring program, Copernicus. The Sentinel-1A SAR operates at 5.405 GHz and supports four imaging modes providing images with different resolution and coverage (Torres et al., 2012). We used the Interferometric Wide Swath Mode (IW) acquisition mode by employing the Terrain Observation by Progressive Scans (TOPS). The IW TOPS mode is the main primary mode of operations for the systematic monitoring of surface deformation and land changes (De Zan and Monti-Guarnieri, 2006). This acquisition mode provides large swath widths of 250 km with a spatial resolution of 5 m x 20 m (IW). The repeat cycle of the twin Sentinel-1A/B constellation is reduced to 6 days.

190 For our analysis, we have acquired two IW Sentinel-1A/B images collected over the study area, in VH polarization along the satellite-descending satellite passes. In particular, we have exploited data acquired after (on November 28, 2016) and before (November 22, 2016) the flooding event (see Table 3).

195 SAR data, provided in the Single Look Complex (SLC) format, have been first radiometrically calibrated in order to convert the digital number (DN) values into corresponding backscattering coefficients, i.e., sigma naught (σ^0) values, which contain information on the electromagnetic characteristics of the surface under investigation. Subsequently, calibrated SAR data have

Commentato [ND1]: This part is changed according to the RC -1 of reviewer 1 and RC -1 of reviewer 3

Formattato: Tipo di carattere: Non Corsivo

Formattato: Tipo di carattere: Non Corsivo

Formattato: Evidenziato

205 been multi-looked with one look in the azimuth direction and four looks in the range one, and finally geocoded, by converting the maps from radar geometry into Universal Transverse Mercator (UTM) coordinates (zone 32T).

After these pre-processing steps, ~~in order~~ to detect land surface changes induced by flooding, we have computed the difference between the post- and the pre-flooding geocoded backscattering coefficient images, and produced the map of the temporal variation of the surface backscattering ($\Delta\sigma^0_{\text{post-pre-flooding}}$).

3.1.2 Multispectral satellite data.

In this category, we considered both low and medium resolution images. Unfortunately, we found co-flood images only for low-resolution images.

210
215
220
225
230
235
240
245
250
255
260
265
270
275
280
285
290
295
300
305
310
315
320
325
330
335
340
345
350
355
360
365
370
375
380
385
390
395
400
405
410
415
420
425
430
435
440
445
450
455
460
465
470
475
480
485
490
495
500
505
510
515
520
525
530
535
540
545
550
555
560
565
570
575
580
585
590
595
600
605
610
615
620
625
630
635
640
645
650
655
660
665
670
675
680
685
690
695
700
705
710
715
720
725
730
735
740
745
750
755
760
765
770
775
780
785
790
795
800
805
810
815
820
825
830
835
840
845
850
855
860
865
870
875
880
885
890
895
900
905
910
915
920
925
930
935
940
945
950
955
960
965
970
975
980
985
990
995

I) **Medium-Low resolution satellite data.** MODIS (Moderate Resolution Imaging Spectroradiometer) is a system of two sun-synchronous, near-polar orbiting satellites called Aqua and Terra that daily acquire images all over the World (Justice et al., 1998). Terra acquires images in the late morning while Aqua in the early afternoon, satellites ~~also have~~ also a night time pass when they acquire in the thermal bands. This repeat frequency does not occur along the same ground track. ~~The ground track~~, and the repeat cycle ~~along the track~~ is every 16 days. ~~This~~ ~~The high revisit time~~ allows detecting with more probability flood over ~~wide~~ vast areas when they still flooded and not covered by cloud. We searched ~~the available for first free-cloud MODIS~~ images from Earthdata portal of NASA (~~https://worldview.earthdata.nasa.gov~~) and we found ~~an~~ (~~https://worldview.earthdata.nasa.gov~~; The selected image ~~of~~ was acquired by Aqua satellite ~~acquired the on~~ 26 November 2016 ~~(The Terra image is too cloudy)~~. We used the 6-bands products with a spatial resolution from 250 to 500 m that range from visible to near-infrared (NIR) and shortwave infrared (SWIR) (Table 4). For the elaboration, we used ~~a spatial resolution of 500 m/pixel~~ the MYD09 - MODIS/Aqua Atmospherically Corrected Surface Reflectance 5-Min L2 Swath 500m, (Vermote, 2015) downloaded from ~~http://ladsweb.nascom.nasa.gov/~~. To have a benchmark of the non-flooded situation, we ~~considered~~ also used the Aqua satellite image of 12 November 2016, which ~~we was~~ compared with the image taken during the flood. ~~We did not apply an atmospheric correction to images, because the MYD09 product is adequate our aim. Moreover, the study area is small (20 km) and the atmospheric parameters for correction available at 1 km of spatial resolution (water vapour, ozone or aerosol) don't show significant change.~~ For the identification of flooded areas, we make the following elaborations:

- a) False colour image made with combinations of 7-2-1 bands for a visual interpretation of flooded areas;
- b) ~~Variation of~~ Modified Normalized Difference Water Index ~~variation~~ MNDWI_{var} (Equation 1). The MNDWI allow detecting water masses or soil moisture. In literature, different combinations for this index are presented and discussed (Xu, 2006; Zhang et al., 2016; Gao, 1996). In our study, we used the ratio between B1 (red band) and B7 (Short

Commentato [ND2]: This part is changed according to the RC -3 of reviewer 1 and RC -1 of reviewer 3

Wavelength Infrared - SWIR). The difference with a non-flooded situation can be used for identifying changes in soil moisture. We used the results of supervised classification to mask the cloud cover.

$$MNDWIvar = MNDWIpost - MNDWIpre \quad \text{where } MNDWI = \frac{(B1-B7)}{(B1+B7)} \quad (1)$$

- c) Supervised maximum likelihood-classification of co-flood image. Supervised classification has already been used in literature to map flooded areas, using machine learning, as described in Ireland et al., (2015). In our work we made a simple supervised classification with SAGA GIS. We first manually defined the training areas with main land use typology visible on the image, and then typologies visible on the false colour image. We try different methodologies for the classifications and we chose as most accurate the maximum likelihood with absolute probability reference and spectral angle methods. We validate the reliability of these classifications with a comparison with false colour image and land-use database. Then, using a GIS query, we extracted the category "area covered by water or wet land/wetland" that mostly correspond to the flooded area. This type of methodology has already been used in literature to map flooded areas as described in Ireland et al., (2015) for accuracy statics reported in result chapter.

II) Medium-high resolution satellite data. Medium-high resolution multispectral satellites (e.g., Sentinel-2 ~~aA~~ and ~~bB~~ or Landsat 8) have a longer revisit time (from 5 days for the Sentinel-2 constellation ~~to~~ ~~16~~ to 16 days for Landsat-8) and it is more difficult to have images at the same time of the maximum flood and cloud free. However, by comparing two images acquired before and after a flood event, it is possible to calculate the variation of different indexes related to change in reflectance of the soil or/and of the vegetation. In this way, it is sometimes possible to map the flooded area indirectly (post-flood mapping). In our study area, we used images taken by Sentinel-2 before the flood (2016, November 11) and after (December 1). Sentinel-2 has some bands at 10-m of spatial resolution and some bands and 20-m of spatial resolution resumed in Table 5. To detect flooded area, we first made a visual interpretation using images with different bands composition of post-flood data. The comparison of considered images allowed ~~to calculate~~ calculating the difference between two indexes:

1. The ~~variation of NDVI~~ (Normalized Difference Vegetation Index ~~—equation 2~~); (NDVI) variation. The NDVI calculated with 10 m of spatial resolution images Sentinel-2 using the near-infrared band (NIR - B8), and the red band (B4). The NDVI is related to the activity of vegetation, and it is possible by calculating its variation (equation 2) to identify the decrease of NDVI values as an effect of inundation on vegetation (Ahamed et al., 2017). Using The detection of this approach, it is possible to indirectly map change allows mapping flooded areas indirectly.

$$NDVIvar = NDVIpost - NDVIpre \quad \text{where } NDVI = \frac{(B8-B4)}{(B8+B4)} \quad (2)$$

Commentato [ND3]: This part was changed on the base of RC - 4 of reviewer 1 and RC -1 of reviewer 3

2. ~~Variation of~~The Modification of Normalized Difference Water Index (MDWI—~~equation 3~~;) ~~variation~~. We use a similar index already tested for MODIS data. We used Sentinel-2 to calculate the MNDWI considering the red edge band (B5) and the SWIR band (B11) at 20 m of spatial resolution. With this approach; ~~(equation 3)~~, it is possible to map the variation soil moisture related to ~~recently~~ flooded areas or areas that are still ~~flooded~~covered by water.

$$MNDWI_{var} = MNDWI_{post} - MNDWI_{pre} \quad \text{where } MNDWI = \frac{(B5 - B11)}{(B5 + B11)} \quad (3)$$

3.2 Flood mapping at local scale with high and ultra-high resolution data

The flood mapping at local scale was made using high and ultra-high resolution images.

270 Immediately after the event, a research project proposed by CNR-IRPI was conducted with the participation of ALTEC S.p.A., Digisky s.r.l. and the Civil Protection Agency of the Metropolitan City of Turin. The aim of the project is a methodological analysis of a possible low-cost solution that could be used for high-resolution mapping of flood effects.

275 The study started from SMAT F2 Project results (Farfaglia et al., 2015), where different solutions for the acquisition of RGB datasets with small and medium Remotely Piloted Aerial Systems (RPAS) were developed. Also previous experiences of CNR IRPI and Civil Protection Agency in the use of small RPAS for the study of geo-hydrological processes (Giordan et al., 2015; Boccardo et al., 2015; Fiorucci et al., 2017; Giordan et al., 2017) were useful for the definition of a correct use of these systems. These previous experiences pointed out how the use of low-cost systems for the acquisition of RGB images and the application of structure from motion algorithm (SfM) can be considered a good solution for the creation of high-resolution 3D models.

280 3.2.1 Aerial high-resolution images

Aerial photo took few hours or within few days after the peak of inundation allow mapping the flooded area with high precision over the most involved territories. In our case, aerial photos were acquired after the flood over the Po river near the village of Pancalieri and for Moncalieri town. We used a low-cost aerial platform (Tecnam P92-JS) provided by DigiSky ~~s.r.l.~~ equipped with Panasonic Lumix GX7 camera (mirrorless with 16 Mp) that allowed to acquire aerial photo with a spatial resolution of 10 cm/pixel. The system ~~has~~ also ~~has~~ an ~~on-board~~onboard GPS that acquires images shooting points and allows the georeferencing of the photos sequence using SfM.

285 The use of manned solution has several add values that can be very useful in this phase: i) it is possible to fly over urban areas without strong limitations that characterized RPAS; ii) the system ~~is able to~~can acquire images over large areas in a limited

lapse of time; iii) the system can flight on demand during the flood ~~efor~~ immediately after (with favourable weather conditions).

The adopted solution was used to acquire 9.2 km² of the most damaged area of Moncalieri and 9.5 Km² of the flooded area of Pancalieri. These two areas are representative of different conditions:

1) The area of Pancalieri is a rural area mainly dedicated to the agriculture. In this case, the Po river flood covered large uninhabited sectors of the Pancalieri plain and reached part of the town of Pancalieri. Here, using SfM, the images of the plane were also processed for the creation of a DSM (resolution of 20 cm) with the aim of mapping geomorphological features related to the flood.

2) The selected area of Moncalieri is a strong urbanized sector of the municipality. In this area there are: i) a motorway, ii) several regional and local streets iii) a residential area with recent unfamiliar houses and small condominiums, iv) an industrial and commercial district. The inundation of this area is due to the Chisola levees breaks. The map of Moncalieri was useful for the identification of most damages elements and in particular the levee. ~~On~~In the most critical areas, we also used ~~also~~ RPAS to acquire ultra-high resolution images.

3.2.2 RPAS ultra-high resolution images

The ultra-high resolution phase is based on the use of RPAS and a terrestrial system. RPAS were used to acquire nadiral photo sequences of the most damaged areas and infrastructures. In particular, we tested the possibility to use RPAS for the identification of damages occurred to the Chisola river levee and one of the most damaged sectors of Moncalieri town. The employed RPAS is a multicopter (CarbonCore 950 octocopter) equipped with a Canon EOS M (Sensor CMOS APS-C, 18Mp).

The system is equipped with a flight terminator and a parachute and can also be used ~~also~~ in inhabited areas. ~~The RPAS was provided by~~ Civil Protection Service of Turin metropolitan area provided RPAS. The obtained aerial photos have a spatial resolution of 3 cm/Pixel. Using SfM, the images of the drone were also used to create 10 cm resolution DSM. All the flood mapping methodology described until now are very often not able to give a consistent measure of water depth. This limitation is not due to the resolution or the time of acquisition, but it is intrinsic in nadiral images. For this reason, in Moncalieri area, we choose to deploy a ground-based solution.

315 3.2.3 Ground-based ultra-high resolution images

As mentioned before, we tested a ~~low-cost terrestrial~~~~low-cost solution~~ system for the acquisition of ultra-high resolution images. In particular, we used an integrated system developed by ALTEC SpA, which couple a Go-Pro HERO 3+ (Black Edition) camera with a GPS and an acquisition module. The system is able to record a STANAG 4609 geolocated HD video. The experimental system was installed over a CNR IRPI car, and a survey was ~~made~~~~done~~ few days after the flood in the considered area of Moncalieri. The continuous record of geolocated video can be a good solution for the acquisition of a ~~large~~~~significant~~ amount of data immediately after the flood when marks of the water level are still clearly visible along building facades. The identification of water level of flooded areas based on the measurement of marks over facades is not a novelty, but the manual acquisition of these data has often been a critical task. Citizens often want to quickly obliterate these signs as a reaction to the critical experience that they lived. The use of field teams that look for these marks can be a time-consuming task that can produce few results with ~~large~~~~considerable~~ efforts also because before the survey it is ~~very difficult~~~~hard~~ to have an idea of the number and the distribution of facades marks that can be identified and measured. The number of marks strongly decreased after few weeks, and for this reason, it is ~~important~~~~essential~~ to have a system that can acquire very fast geolocated images and that can be easily used over large areas.

The presented system is ~~very simple~~~~straightforward~~ and ~~effective~~~~efficient~~. The geolocated video can be analysed by other components of the team immediately after the acquisition or after many days. The ~~important~~~~primary~~ goal is the fast acquisition of numerical information of the flood effects that can be used for several purposes. For the identification and mapping of water levels, the video is analysed and a frame sequence is extracted from it when the operator sees some marks lefts by water over facades. The developed system is able to extract not only frames but also their geocoding information, which are computed using SfM applications. The result is a georeferenced 3D model of the façade that can be used to measure the water level with a good approximation (few cm). We validate the accuracy measures of water level based on SfM with manual measures accurately geolocated with GPS RTK positioning.

3.2.4 Field data

Field survey, ancillary data like a measure of ~~groundwater~~~~river~~ discharge stations, and civil protection reports were used to validate the maps derived from remote sensing interpretation and the simulation models for Pancalieri and Moncalieri areas. We made a GPS RTK campaign in Tetti Piatti and Tagliaferro areas to have direct measurements of flood marks. In particular, we acquired the 3D position of marks previously identified using the available video. We used third part materials like

newspaper reports, photo and videos found on the web with a validation of their reliability ~~in terms of regarding~~ geolocation and time. Available data were used to check the extension of flooded area and water height mapped with other methodologies.

3.3 Water depth models based on DTM approach.

As mentioned before, the ~~main primary~~ goal of the presented methodology is the definition of the maximum depth reached by the water during the flood. The map of water maximum depth (WD) is an important document that can be used for ~~the~~ first definition of damages and remedial actions. All the acquired material, and in particular data that define the water depth reached by the flood, were used to calculate the water maximum depth map. In our study, we adopted a simple raster-based model (Bates and De Roo, 2000) and we created ~~a water an~~ absolute water level (WL) raster. The first step is the ~~definition of WL is~~ the acquisition of several measure points of water level (WL_p) that are ~~provided by~~ calculated from the ~~estimation of measured~~ water depth point (WD_p). WD measures can be done using: i) georeferenced photos (low accuracy); ii) ultra-high resolution ~~phase results (high accuracy); iii) direct measurements supported by measure derived from SfM and integrated with manual~~ measure geolocated GPS RTK positioning; ~~iv (high accuracy); iii) civil protections reports (the level of accuracy can be very different); v); iv) data acquired by hydrometric river level monitoring stations.~~ Starting from the collected ~~punctual spotted~~ measures and the 5-m LIDAR digital terrain model (DTM) freely provided by Regione Piemonte, we calculated the WL value for each point using a simple formula: $WL_p = DTM + WD_p$. Available WL points were used to create the water level contour lines and then interpolated using GIS software to obtain the raster of WL gradient. The WL raster is used to create the raster map of water depth which can be calculated with a simple raster calculator of ~~a~~ GIS software using the reversed formula $WD = WL - DTM$. WD ~~maps map~~ is ~~an important necessary~~ information to assesses and improve the limit of the flooded area and, it is also fundamental for the phase of preliminary damages assessment. We produced maps of water depth at medium resolution for Po river (Fig. 5) and ~~at~~ high resolution for Moncalieri (Fig. 11) and Pancalieri area (Fig 6).

4 Results

4.1 Flood mapping from low to medium-high resolutions with satellite data.

The satellite data allowed ~~to map mapping~~ the flooded areas by Po river, ~~Chisola~~ Chisola and Oitana stream, with a resolution that ranges from 500 m of MODIS to 10 m of Sentinel-2. In following figures (Fig.3. Fig 4. and Fig.5), raster maps based on remote sensing maps data are compared with our limit perimeter of the flooded area (black polygon). ~~The flooded area limits~~ were We manually extrapolated the flooded area perimeters considering both satellite data and geomorphological features

370 ~~obtained using observed in the hillshade model derived from 5-m DTM of Regione Piemonte and used as a benchmark for.~~
~~For the evaluation of the performance automatic flooded area maps based on satellite data, we applied a GIS query for each~~
~~map to create boolean rasters of remote sensing analyses. flooded / not flooded area. Then we overlapped the obtained raster~~
~~with manual polygons for a geo-statistical analysis, for each polygon is reported the percentage pixel classified as flooded/not-~~
~~flooded. The main results are reported in table 6.~~

375 For Po and part of Chisola, the flooded areas were also mapped also with the help of ~~water height simulation on the base of WFD~~
~~model based on~~ DTM. At the moment of writing this paper (November 2017), it is still not available an official delimitation
of flooded areas, a map made by ARPA Piemonte is under validation, and the data will be published in the next months. ▲

Commentato [ND4]: This part is changed according to the RC -8 of reviewer 1

Formattato: Tipo di carattere: Times New Roman, Non Grassetto

4.1.1 Flood mapping with SAR data

380 I) Co-flood mapping with COSMO-SkyMed data. Results of data classification are reported in Figure 3A, where four main
classes, i.e., water/flooded (blue), soil/vegetation (green), urban (pink) and quarry lake from ancillary data (cyan), are shown.
The analysis could not detect all flooded areas because the COSMO-SkyMed data was acquired in the early morning of 25
November while the phase of the maximum flood of Po river occurred on 25 November afternoon. At the time SAR data was
385 acquired (05:05 UTC), the Pancalieri area was at initial stage of flooding and the urban area of Moncalieri was not flooded yet
(the flooding in this area started a few hours later). Only the Oitana stream already flooded over most of the areas. It is important
to note that, in the COSMO-SkyMed image, some areas classified as water are not flooded zones but quarry lakes. Accordingly,
the analysis based on COSMO-SkyMed data cannot provide an exhaustive flood map but results may be considered satisfactory
in terms of spatial distribution of flooded areas.

390 I) I) Co-flood mapping, reclassified amplitude of COSMO-SkyMed data. Results of image classification are shown in Figure
3A, where three classes of SAR amplitude were defined by means of empirical thresholds: i) low that correspond to water
covered area (blue); ii) intermediate like soil/vegetation (green); iii) high that are urban areas (pink). In the figure are also
overlapped the quarry lake from ancillary data (cyan). The accuracy in the correct detection of land-use type is quite good
ranging from 80 % for soil and vegetation, 67% for urban area to 61% for water body (tested in quarry lakes). Vegetation and
395 buildings are factors that reduce the detection of water covered areas even using full-resolution images and more complex
processing (Pierdicca et al., 2018). In a second step we selected with a GIS query the low resolution (water covered) class that
mostly correspond to the inundated areas and we compared with the real flooded area. Also the accuracy in the correct detection
of flooded areas is quite good: it ranges from 57 % in the lower Oitana stream to 2% in the Po area near Moncalieri. This is
related to the time of satellite acquisitions (05:05 UTC of 26 November 2016) some hour before the flood peak. The flood

400 wave positions can be appreciated especially along the Po river, where upstream (near Pancalieri) about the 42% of flooded area was detected, while downstream (Carignano) decrease to 4%. The urban area of Moncalieri limits the capability detection of inundated areas. The false positive errors are less than 5% of the area.

405 II) Post-flood mapping with Sentinel-1 data. Figure 3B shows the map of the post- pre-flood SAR backscatter difference ($\Delta\sigma^{\circ}_{\text{post-pre-flooding}}$) where the application of empiric thresholds allowed us detecting areas covered by water, i.e., flooded ($\Delta\sigma^{\circ} < -1\text{dB}$). Such results show that most of the areas classified as flooded by the co-flood analysis were not anymore covered by water on 28 November 2016. Only small depressed areas, e.g., ancient meanders of Po river, were still flooded, as shown in Figures 3D', 3D'' and 3D''' (the areacase of Pancalieri, discussed more deeply in par 4.2.).

4.1.2 Flood mapping with multispectral data

410 I) **Multispectral low resolution, MODIS-Aqua.** The MODIS-Aqua satellite takestook an image quitereasonably free of clouds over the entire Piemonte during the late morning of November 26, 2016. The image allowed ~~to detect~~detecting the flooded areas with a resolution of 500 m.

415 From the false colour images (Fig. 4 B), even if the area at the south of Turin is not yet directly flooded, it is only possible to detect that the soil was saturated of water (dark green-blue in false colour composition). The identification of flooded area is more evident from theThe comparison with pre-flood image of November 12, 2016 (Fig. 4-A): 4 A) improved the detection of the flooded area.

We also try to extract in an automatic way the flooded area: with the equations previously described:

420 In figure 4 C we identified flooded area using a GIS query with the value $MNDWI_{\text{sat}} \geq 0.3$. This value is an empirical threshold that allows selecting most of flooded area and minimizes false positive errors. The results show a good correspondence between the area-manually drawn and the area-automatically classified even ifflooded area, however around 35% of the flooded area was not correctly-identified. ThisThe mismatch can be explained ifwith the satellite passedacquisition at the end of the co-flood stage- when water started to withdraw. It is also possible to see some false positive pixels (<10 %) that correspond to the shadow of the clouds even if clouds were partially filteredor haze that was not possible to entirely filter.

425 In figure 4 D shows the maximum likelihood-Supervised Classification. We also made a supervised classification of eo-flood 26 November MODIS image: using maximum likelihood (MLC) (Fig. 4 D) and spectral angle (SA) (Fig. 4 E) methods. In the study area, we classified four mainprimary land cover: vegetation, bare soil, cloud, and water body / wet soil that shouldalmost identify the flooded area. Supervised-sector (the water bodies likes the quarry lakes are too small for MODIS pixel). After a visual checking of the classification identified most of the floodedreliability, we used a GIS query to select the "water covered

Commentato [ND5]: This part was changed on the base of RC-2 of rewiver-2 and RC-1 of rewiver-3

and wet areas ($> 80\%$) but with more false positive cases that correspond to cloud shadow” classes. The query creates a boolean raster of flooded areas classified as water. The accuracy of flood map based on supervised classification is good: it identifies most of the flooded areas for Po river ($> 70\%$) with low false positive pixel (table 6). Worst results for the area flooded by Chiosla and Oitana.

For both indexes, it is possible to see that the area town of Moncalieri (red square 1 in figure 34) flooded by Chiosla stream is not well identified.

II) Multispectral medium-high resolution post-flood mapping Sentinel-2. The images of Sentinel-2 were analysed by visual interpretation of RGB composite image and using two different indexes (NDVI – MNDWI) to identify flooded areas shown in figure 5. For both indexes we used a GIS queries with empirical thresholds to extract the flooded area:

1) NDVI variation ($NDVI_{VAR}$) at 10 m of Spatial resolution (Fig. 5 A). The results show that for Po, Chiosla and Oitana a clear pattern of negative NDVI variation corresponds to the flooded area. The study area is almost flat and mostly occupied by cultivated fields and, in November, it was characterized by tillering of wheat. The flood caused a deposition of a thin layer of silt sediment that caused a decrease of vegetation activity (most of the flooded area shows an $NDVI_{VAR} < -0.06$) that could be detected using the available dataset. By the contrary, the wheat field outside flooded area shows an increasing or stationary NDVI. In the maps are visible negative $NDVI_{VAR}$ also outside the flooded area that is related to: i) winter decreasing of activity of natural vegetation or some type of cultivations, ii) longest building shadow in urban areas. The presence of false positives hampers the use of automatic classifications of flooded areas, and a visual interpretation is necessary. It is possible that flood effects and the layers of silts could have also affected also the crop productivity with relative economic damages as reported in other cases (Tapia-Silva et al., 2011; Shrestha et al., 2017), but this evaluation is not the aim of this study.

2) MNDWI variation ($MNDWI_{VAR}$) at 20 m of spatial resolution. The index is directly related to the presence of water or high soil moisture. The results show that for Po, Chiosla and Oitana areas floodplain (Fig. 5 B) a clear pattern of positive $MNDWI_{VAR}$ that indicates an increase of soil moisture and the presence of some areas that were still inundated. It is possible to see that a threshold of $MNDWI_{VAR} + 0.1$ is the best to delimit the flooded areas. However, like for NDVI, the presence of many areas with positive variations outside the flooded sector makes more accurate a manual interpretation with respect compared to an automatic classification. The evidence also suggests that for this index it is important to have images taken within few days after the flood when the involved affected areas are still covered by water or with soil very wet. In table 6 are resumed the accuracy statistic for automatic mapping of flooded or very water saturated areas based on satellite data: MNDWI show little better accuracy than NDVI. It is worth to note that for Sentinel-2 for both $MNDWI_{VAR}$ and $NDVI_{VAR}$ the flooded area is well detectable in the local area around the village of Pancalieri ($> 50\%$ of accuracy) where land use is mostly cultivated land, while

Formattato: Titolo 4, Allineato a sinistra

Formattato: Giustificato

is more difficult to detect the flooded ~~are~~area in the ~~ease~~high urbanized town of Moncalieri ~~that is mostly urbanised~~ (<20% of area detected).

460 **III) Water depth model.** ~~The water depth~~We create WD model for Po river ~~was created~~ following the procedure described in paragraph 3.3, ~~the~~ The results are shown in figure 5C. The simulated WD model has a ~~very~~ good match with benchmark polygon and the evidence from Sentinel-2 (Fig. 5 A and B), MODIS data (Fig. 4). It is also possible to observe some discrepancy at South-East of Moncalieri where large area should be flooded according to model but in reality, was not affected.

465 This mismatch could be explained by the presence of artificial structures (e.g., embankment) that protect flood-prone areas and our model cannot ~~be simulated~~simulate. The uncertainty of our WD model is complicated to evaluate because it depends on many factors: the main limits is the number of ground-based WD measures, their reliability and their geolocation. The interpolation to obtain water table is also another source of error. The Lidar DTM of Regione Piemonte accuracy in our model elevation is range from +/-0.3 m to +/- 0.6 m in urban areas. Over this ~~large~~vast area we have not ground measure for validation, but it is possible to estimate from some photos found on the web that model error is withinabout 0.5 m. In the ~~higher~~ high-resolution WD model of Pancalieri and Moncalieri shows in the next chapter was possible to validate data with ground truth evidence.

470 The final limits of the flooded area are the results of both remote sensing and WD model interpretation ~~its~~. Its accuracy can be considered goodacceptable for large cultivated area and large flooded area by Po river but less accurate for urban ~~area~~zone especially in Moncalieri where a local high-resolution analysis is needed to quantify the severity of the flood.

4.2 Flood mapping at local scale with high-resolution data.

480 Inside the area analysed using remote sensing systems, we choose the most critical sectors of Moncalieri and Pancalieri to test high and ultra-high resolution images. As mentioned before, the high resolution has been acquired using an aircraft, ~~and~~ the ultra-high resolution using RPASs and a ground-based ~~photo-system~~photosystem. All the images have processed using SfM that allowed to obtain ~~ortho~~photo~~ortho~~photo and 3D models.

4.2.1 High-resolution aerial photo-~~2~~ Pancalieri

485 ~~The Po river partially flooded the~~ village of Pancalieri ~~was partly flooded by Po river in~~on the morning of November 25, 2016. This area has also been mapped ~~also~~ by high-resolution aerial photo (10 cm/Pixel) ~~in visible, RGB bands~~ provided by DigiSky. Aerial photos were taken November 28, 2016 (figure 6 A) and allowed to refine the map of the flooded area form

the medium resolution maps obtained with the interpretation of Sentinel-2 data. With the help of digital surface models (DSM) at 0.2 m of spatial resolution derived from SfM, we also ~~mappe7d~~~~mapped~~ geomorphological features like erosion (meanders cut) and deposition areas and road damages (Fig. 7 C). The integration of aerial photo and DSM ~~also allowed also to~~ ~~make~~~~making~~ a 3-D model where it was possible to measure water depth for some points where water level marks are well detectable (Fig. 7 B).

Using the procedure described in paragraph 3.3 we produced a WD model for the Pancalieri area (Fig. 6 D) with higher accuracy respect to the rest of Po valley. The higher accuracy of the model was obtained using: i) high-resolution aerial photos ii) spot measures derived from SfM iii) different video and photos found on the web and geolocalized with the help of Google Street view (e.g., Fig. 6 B and 6C). The model shows that part of the Pancalieri village was flooded by a modest height of water (< 0.5 m) while near Po river WD reached 2-3 m with a ~~strong~~~~fast~~ flow that caused erosion channel. From the map of the flooded area (Fig. 6 D) it is also interesting to note that, during the flood, ancient meanders at the east of Pancalieri were reactivated and ad consequence some areas were flooded quite far from Po main course.

Some months after the flood (April 2017), satellite photos available on Google Earth (0.5 m spatial resolution) still show some trace of flood like erosions and area covered by sand deposits. The flooded area is much more difficult to identify and confirm the importance to acquire data as soon as possible after a flood event.

4.2.2 High-resolution aerial photo and ultra-high resolution RPAS 3D models - Moncalieri.

Some parts of Moncalieri municipality (Tetti Piatti, Carpice and Tagliaferro localities) were flooded in the late morning of 25 November by Chisola stream that breached its embankment in different points (Fig. 8 B). On the left side of Chisola, the area with a very dense residential and industrial settlement suffered ~~strong~~~~severe~~ damages. Hundreds of people were evacuated. In the evening of November 25, ~~Po river flooded~~ another sector of Moncalieri municipality ~~was flooded by Po river~~.

Few days after the flood, the area flooded by Chisola was analysed with different methodologies:

1. High-resolution aerial photos. Like in Pancalieri, on November 29 a very high resolution (0.1 m/pixel) aerial photo using the aerial platform of DigiSKY was taken over an area of about 9.2 km². The aerial photo allowed to refine the map of flooded areas (Fig. 8 A) and to detect the points where river embankment collapsed (Fig. 8 B).
2. Ultra-high resolution RPAS photos. On December 3, 2016, RPAS ~~acquired~~ photos (resolution of 0.02 / 0.03 m/pixel) ~~were~~ ~~aequired~~ over some most critical areas (e.g., Tetti Piatti – Fig. 8 C) for precise-a mapping of flood effects. In this area, ultra-high resolution allowed to detect some damages like the toppling of a wall in recently built urbanization or the waste accumulation derived from damaged objects ~~originally~~~~initially~~ located in houses or industrial warehouse. The presence of

515 these deposits is a clear evidence of the occurred damages, but also a confirmation that nadiral images are not able to supply a sufficient dataset for the identification and evaluation of damages in urban areas.

520 The DSM based on RPAS photos ~~also~~ allowed ~~also~~ to create a detailed 3-D model of river embankment rupture (Fig. 9). The presented 3D model confirmed that the level of Chisola during the flood was very critical with a difference of fewer than 0.5 m ~~with respect to/from~~ the top of the levee. The ~~water~~-maximum ~~water~~ level considered under the security limits suggested by Po river authority is 1 m ~~with respect to/concerning~~ the top of the embankment. The RPAS model ~~also~~ allowed ~~also~~ to map geomorphological effects of the rupture of the embankment. In particular, figure 8B and figure 9 show a ~~strong~~massive erosion ~~of field~~ near the break and a pseudo alluvial fan created by the flow of water.

4.2.3 Measure of water depth with SfM model from terrestrial camera, Moncalieri.

525 In the same days of UAV an aerial photo ~~campaigns~~campaign, a field survey using an integrated system provided by ALTEC S.p.A. installed on a car (Fig. 10 B) was made in the same urban areas of Moncalieri flooded by Chisola (Fig 10A). The survey had the aim of measuring the maximum water level reached and made a rapid evaluation of damages. The survey last about 1h for 12 ~~kms~~km of the path along the road of the most critical area hit by the flood.

530 Where the level reached by the water was still visible over several facades, (Fig. 10 C and Fig.10 D) it was possible to ~~make an estimation of/estimate~~ the maximum water level of the flood. During the first survey, we found 11 points where watermarks over facades were still visible. During the post-processing, we realized that the quality of the images extracted from the video was insufficient for the SfM application: the bitrate was too low and the frames are too pixelated. For this reason, after a month we performed a second survey with a higher bit rate along the same path, but only ~~6~~six marks still visible (Fig 10 A).

535 This reduction of available points confirmed that the delay between the flood and the survey is a fundamental element that should be carefully considered because the number of possible information decrease exponentially. For this second terrestrial camera acquisition, an improvement of the encoding quality was introduced. Such improvement allowed the extraction of ~~good~~high quality images compatible with SfM application. We obtained 3D models of the surveyed sectors, and we measured the high of water marks on façades. Then we validated the information obtained from SfM with a manual water height measurement geocoded with GPS Rtk systems for the 6 points and ~~for~~ other additional 5 points. The accuracy of measurement considering that is a low-cost solution and one of the first experimental tries for this system is ~~very good~~excellent; the average error compared SfM water level measurement with manual measure can be estimated in few centimetres (see table ~~67~~).

Commentato [ND6]: This part was changed on the base of RC-9 of rewiver-1

4.2.4 High-resolution water depth models and ancillary data for damages evaluations – Moncalieri.

The combined use of measures derived from: i) car camera elaborated with SfM, ii) manual GPS RTK, iii) the hydrometric level of Chisola stream registered by ARPA Piemonte station (Fig. 11 B) represents a gooduseful dataset for the estimation of the WD. Using the 5m DTM Lidar of Regione Piemonte, we obtained the WL and the WD rasters (Fig. 11 A). The result shows that in a large part of the analysed area, the water height was between 0.5 and 1 m. Unfortunately, in some morphological depressions, the level was higher than 1.5 m. The model also shows that in the cultivated area close to left Chisola embankment water probably reached 2 -3 m height.

The water level map can suffer from some errors from pointualspot measure these. These are related to the quality of DTM, or the effect of local structures that can modify the water flow and height at a local scale. The comparison of water level measured with SfM / GPS and calculated level with DTM show variation within 0.2 m that is a good result (Table 6).

Ancillary data like photos or video found on the web (local newspaper, social media) and geolocated with Google Streetview allowed to improve and validate the map of flooded areas and the height of the water (Fig 11 C). On the web, it is possible to find a lot of photos or video of the flood event, but only small part of them can be geolocated with goodadequate precision and validated.

The water height map was crossed with buildings database of Regione Piemonte to assign to each building the average of water height reached by the flood (Fig 12 A). The water height is one of the mainleading parameters that can be used for a preliminarypreliminary estimation of potential damages. We divided the water height in 3 main classes corresponding to low (<0.5 m), medium (0.5 – 1.5) and high (> 1.5) damages expected. These thresholds have been empirically defined by Luino et al. (2009) and Amadio et al. (2016). The obtained map is a good representation of the level of damages caused by the flood that could be considered the final product of the presented methodology.

This result was compared with ground data where possible: for instance, in the industrial warehouse shows in detail map in figure 12 B was estimated an average value of 0.8 m water level (medium degree of damage expected). The evidence from a geolocated photo from La Stampa newspaper confirms this value.

4.3 Flood mapping strategy flowchart

The flowchart in figure 13 shows the approach that we propose for the choice of instruments and methods to map the flooded areas, based on the results of this study. If free satellite data are available, it is possible to sort them taking into account the parameters of time elapsed from flood and the spatial resolution.

I) The priority is to search for co-flood images that allow an easy mapping. In case of night and cloudy conditions it is necessary to use SAR image (Sentinel-1) while for multispectral data acquired during the day the choice is related to spatial resolution: for instance, Sentinel-2 or Landsat-8 data are more resolute than MODIS data.

II) In the case we have post-flood satellite pass only multispectral data can be used. Also for post-flood data, the spatial resolution and time elapsed from the flood are the parameters that should drive the choice. The use of post-flood data implies more complicated post-processing (e.g., bands index variation) and with the support of ancillary data and DTM to extract the flooded area map. In general, the rapid access to data portal of free satellite data allows to download the data and to make an evaluation of the best solution for the case under study, that not necessarily is the data with high spatial resolution.

After this step it is possible to make a first delimitation of flooded areas, that in case good data may be an already corrected and ready to use map. Then it is possible to focus the acquisition of on-demand of high-resolution sensors only in the most critical or unclear areas (case 2A). If we use only on-demand data, without rapid satellite mapping, we could map large area at high spatial resolution (case 2B). This solution, however, implies a higher cost. In case of direct mapping at very-high resolution, it is better to use low-cost aerial platforms that are more flexible respect to on-demand commercial satellites. The integration with DEM data allows creating the water depth model at basin scale and a further refinement of flooded area maps (2C).

Urban area flood mapping (3) can be considered a hotspot priority inside the general flood map. It needs a more accurate and high-resolution mapping with use of ground-based measures (like SfM model based on car photo), RPAS survey, and the creation of a water depth model that is essential for a precise flood magnitude assessment.

It is important to remind that is not possible to select a priori which type of data/processing is the better for flood mapping. The best method to use depends on different factors: 1. Satellite acquisition and time elapsed from flood peak; 2. Type of satellite data (SAR / multispectral, spatial resolution); 3. Study area features and risk (dimension, cloud cover, land-use and element at risk); 4. Affordable cost (e.g., we use commercial satellite data or traditional aerial photo only if they give significant advantages to flood mapping).

5 Discussion and conclusions

In this work, we tested different methodologies for a low-cost and rapid flood mapping and characterization/water depth assessment using the November 2016 Piemonte flood as a case history. We used a multiscale and multi-sensors/sensor approach in order to know pros and cons of each methodology in relation to about the site conditions and available data-. We also proposed a flowchart model to map flooded areas from satellite to ground-based data.

Commentato [ND7]: This paragraph was added following the comments RC 4 of reviewer 3 and RC 12 reviewer 1

Formattato: Tipo di carattere: Non Grassetto

At the regional scale, satellite remote sensing showed a good performance in the flood mapping: the combined use of InSAR/SAR data of Sentinel-1 and Cosmo, and multispectral data of MODIS-Aqua and Sentinel-2 allowed creating maps of the flooded area. The maps of flooded areas automatically extracted from remote sensing data were used with the help of DTM and water depth model as a base map for an accurate manual drawing. In our study area (320 km²) about 66 km² was flooded by Po river, Chisola and Oitana streams. WD models show that some areas were flooded up to 2 m of water height.

InSAR data showed a good performance in the real-time flood mapping while are weaker for post-event mapping. By considering the obtained results. Concerning SAR data, we reclassified a simple preview low-resolution Cosmo-Skymed amplitude image acquired some hours before the co-flood time. The results show that the time of satellite pass is fundamental: if the area is covered by water (like upstream part of Po river) up to 60% of pixels was correctly classified as flooded and it was possible to observe a clear pattern. We compared pre- and post-flood SAR images of Sentinel-1 making SAR backscattering difference of radiometrically calibrated images. The result shows that SAR is weaker for post-event mapping: in our case 3 days after the flood (Sentinel-1) less than 4% of the flooded area is still detectable. By considering the obtained results, it is also clear the importance to have free and constant SAR satellite data provided by national agency: a short revisit time and a constant acquisition are factors that increase the probability to have SAR image for real-time flood mapping. For instance, the two Sentinel-1 provide free images every 6six days, while other satellites have quite high costs and the acquisition of the extra images is activated with emergency procedure acquisition like the EMSR of the European Union or by civil protection authorities that not always provide useful maps for whole damages assessment.

MultiThe low-resolution MODIS image acquired near the co-flood stage allowed a good identification of flooded areas using different methods: MNDWI variation and supervised classifications. The detection accuracy is good especially for the area flood by Po river where about the 70% of the flooded area was correctly identified.

Medium-High resolution multi-spectral data have more capability with post-event images. In this work, we tested NDVI and MNDWI variations for the detection of flooded areas based on the comparison of pre- and post- event images. Both methodologies show quite good-performance in cultivated land, while(40 % - 45% of accuracy). Here it is more possible to detect a clear pattern: inside the inundated area the percentage of pixel classified as flooded is four times greater than in not flooded area. The inundated areas are more difficult to detect in the interpretation of images for dense urban areas-area of Moncalieri (only 4% area was correctly mapped). Water depth model and DTM gave an important help in the improvement of flooded area of Po river based on remote sensing data. In last years, the revisit time for free multispectral data has been strongly was sharply reduced (Landsat-8 has a revisit time of 16-days and Sentinel-2 fof 5 days from march March 2017 with the launch 2nd second satellite). This increase the probability to have an image free of cloud within few days or weeks after the

Commentato [ND8]: This part was changed according to RC-3 of reviewer 2

flood or in some cases during the inundation phase. At the local scale, flood mapping showed a good agreement with regional scale mapping.

~~At local scale, flood mapping showed a good agreement with regional scale mapping.~~

630 The high-resolution aerial photo and ultra-high resolution aerial photo from RPAS allowed ~~to map~~ mapping flooded areas with more precision. The application of Structure from Motion (SfM) allowed creating high-resolution DSM useful to map the geomorphological effects (e.g., meanders cut) and the ~~main~~ widespread damages (embankment rupture) in Pancalieri and Moncalieri area.

635 ~~For~~In the ~~considered~~ urban area (of Moncalieri), where satellite data ~~is weaker~~ have low accuracy and a precise evaluation of water height/depth is ~~very important~~ necessary for flood damages evaluation, the solution is the ~~aequisition of~~ integration with ground-based data. In our work, we tested a low-cost solution with a GO-PRO HERO 3+ (Black Edition) camera installed on a car that allowed to make 3D models and to measure the water height reached during the flood. These measures validated with GPS showed ~~a good accuracy~~ good accuracy, but it is necessary to do the survey within few days after the flood when ~~many water signs~~ are visible. A proposal for the future is to use this system during the emergencies, for instance, on civil protection car, to have a map of water depth with a much higher density of points.

640 ~~A possible idea is to use this system during the emergencies, for instance, on civil protection car, in order to have a map of water height with much higher density of points.~~

645 Using these measures and a high-resolution DTM, it was possible to generate a raster model of water depth that has a good match with the ground truth and could be used about +/- 0.2 m of accuracy. We used the results of WD model for the a preliminary evaluation of building damages or. The model could also be used in the future for flood prevention policy. This model can be also used for the estimation of the degree of damage for every building located in the flooded area. or civil protection plans.

Finally, from our work it is also clear the importance to collect ancillary data also from the new sources on the web: the photo and video collected during the flood by simple citizens can be a precious help for the validation of flooded area maps.

650 Data availability.

MODIS data were downloaded from ~~Worldview~~NASA LAADS - DAAC portal (<https://worldview.earthdata.nasa.gov/>) (<http://ladsweb.nascom.nasa.gov/>) link retrieved 21-11-2017-16-02-2018 12/11/2016: ~~MYD09GAM~~MYD09.A2016317.h18v041215.006.2016319100800 view: <https://go.nasa.gov/2ymajYe2016319043220>

Formattato: Colore carattere: Colore personalizzato(34;34;34)

655 26/11/2016: ~~MYD09GA.A2016331.h18v04.006.2016333055328~~ ~~view~~
~~<https://go.nasa.gov/2y4keBY>~~~~MYD09.A2016331.1225.006.2016333031908~~

Formattato: Colore carattere: Colore personalizzato(34;34;34)

Sentinel data- were download from Copernicus Scihub: <https://scihub.copernicus.eu/> -link retrieved 21-11-2017

Sentinel-2:

660 1/12/2016: S2A_OPER_MSI_L1C_TL_SGS__20161201T104644_20161201T141912_A007541_T32TLQ_N02_04_01
8/11/2016: S2A_OPER_MSI_L1C_TL_SGS__20161108T103641_20161108T154744_A007212_T32TMQ_N02_04_01

Sentinel-1:

28/11/2016: S1A_IW_GRDH_1SDV_20161128T053526_20161128T053551_014138_016D3F_7094
22/11/2016: S1B_IW_GRDH_1SDV_20161122T053445_20161122T053514_003067_005376_AD1

665 ~~Cosmo-Skymed [quiklook image data portal](#) (E-Geos <http://www.e-geos.it/>)~~

~~Image ID_ 627100~~ acquired on 25 November ~~2016 05:11 UTC~~ COSMO-SkyMed© ASI [2016] ~~<http://catalog.e-geos.it/#product:productIds=627100>~~ link retrieved 16-11-2017

Formattato: Italiano (Italia)

Formattato: Italiano (Italia)

Formattato: Italiano (Italia)

Formattato: Italiano (Italia)

Formattato: Italiano (Italia)

670 5-m LIDAR- DTM Regione Piemonte is available at:
~~<http://www.geoportale.piemonte.it/geonetworkrp/srv/ita/metadata.show?id=2552&currTab=rndt>~~ link retrieved ~~21-11-2017~~~~16-02-2018~~

Formattato: Colore carattere: Automatico

Acknowledgments.

675 The authors gratefully acknowledge Italian Space Agency (ASI) and E-GEOS -for the permission of free use of- Cosmo-Skymed quick-look data. -ARPA and Regione Piemonte for the ~~support in the search of~~ meteorological and hydrological data ~~of 2016 flood event~~.

Reference

Commentato [ND9]: Reference revised according to editor comment

680

Ahamed, A., Bolten, J., Doyle, C. and Fayne, J.: Near Real-Time Flood Monitoring and Impact Assessment Systems, In Remote Sensing of Hydrological Extremes (pp. 105-118) Springer International Publishing, doi: 10.1007/978-3-319-43744-6_6, 2017.

Amadio, M., Mysiak, J., Carrera, L. and Koks, E.: Improving flood damage assessment models in Italy, Nat. Hazards, 82(3), 2075-2088, doi: 10.1007/s11069-016-2286-0, 2016.

~~Arrighi, C., Brugioni, M., Castelli, F., Franceschini, S. and Mazzanti, B.: Urban micro-scale flood risk estimation with parsimonious hydraulic modelling and census data, Nat. Hazard Earth Sys., 13(5), 13, 1375-1391, <https://doi.org/10.5194/nhess-13-1375-2013>, 2013.~~

ARPA Piemonte: Evento alluvionale 21-26 novembre 2016 – rapporto preliminare [\(Italian\)](#), 21-25 November flood event preliminary report, Available at http://www.arpa.piemonte.gov.it/publicazioni-2/relazioni-tecniche/analisi-eventi/eventi-2016/rapporto-preliminare-novembre-2016-def.pdf/at_download/file (accessed 1-0812-2017), 2016.

~~Arrighi, C., Brugioni, M., Castelli, F., Franceschini, S. and Mazzanti, B.: Urban micro-scale flood risk estimation with parsimonious hydraulic modelling and census data, Nat. Hazard Earth Sys., 13(5), 13, 1375-1391, <https://doi.org/10.5194/nhess-13-1375-2013>, 2013.~~

Barredo, J.I.: Major flood disasters in Europe: 1950–2005, Nat. Hazards, 42(1),125-148, doi: <https://doi.org/10.1007/s11069-006-9065-2>, 2007.

Bates, P.D. and De Roo, A.P.J: A simple raster-based model for flood inundation simulation, Journal of Hydrology, (236), 54–77 doi: [https://doi.org/10.1016/S0022-1694\(00\)00278-X](https://doi.org/10.1016/S0022-1694(00)00278-X), 2000.

Bignami, D.F., Rulli, M.C. and Rosso, R.: Testing the use of reimbursement data to obtain damage curves in urbanised areas: the case of the Piedmont flood on October 2000., Journal of Flood Risk Management., doi: <https://doi.org/10.1111/jfr3.12292>, 2017.

Boccardo, P., Chiabrando, F., Dutto, F., Tonolo, F.G. and Lingua, A.: UAV deployment exercise for mapping purposes: Evaluation of emergency response applications. Sensors, 15(7), pp.15717-15733, doi: <https://doi.org/10.3390/s150715717-2015-15737>, doi:10.3390/s150715717, 2015

~~Brakenridge, R. and Anderson, E.: MODIS based flood detection, mapping and measurement: the potential for operational hydrological applications. Transboundary floods: reducing risks through flood management, 1-12, doi: <https://doi.org/10.1007/1-4020-4902-1-1>, 2006.~~

710 Boni, G., Ferraris, L., Pulvirenti, L., Squicciarino, G., Pierdicca, N., Candela, L., Pisani, A.R., Zoffoli, S., Onori, R., Proietti, C. and Pagliara, P.: A prototype system for flood monitoring based on flood forecast combined with COSMO-SkyMed and Sentinel-1 data, *IEEE ~~J-SEL-TOP-APPL~~Journal of Selected Topics in Applied Earth Observations and Remote Sensing*, 9(6), pp.2794-2805, doi: <https://doi.org/10.1109/JSTARS.2016.2514402>, 2016.

Brakenridge, R. and Anderson, E.: MODIS-based flood detection, mapping and measurement: the potential for operational hydrological applications. Transboundary floods: reducing risks through flood management, 1-12. doi: https://doi.org/10.1007/1-4020-4902-1_1, 2006.

715 Brivio, P.A., Colombo, R., Maggi, M. and Tomasoni, R.: Integration of remote sensing data and GIS for accurate mapping of flooded areas, *International Journal of Remote Sensing*, 23(3), 429-441, doi: <https://doi.org/10.1080/01431160010014729>, 2002.

Buzzi, A., Tartaglione, N. and Malguzzi, P.: Numerical simulations of the 1994 Piedmont flood: Role of orography and moist processes. *Monthly Weather Review*, 126(9), pp.2369-2383, doi: [https://doi.org/10.1175/1520-0493\(1998\)126<2369:NSOTPF>2.0.CO;2](https://doi.org/10.1175/1520-0493(1998)126<2369:NSOTPF>2.0.CO;2), 1998.

720 Carraro, F., Collo, G., Forno, M.G., Giardino, M., Maraga, F., Perotto, A., Tropeano, D.: L'evoluzione del reticolato idrografico del Piemonte centrale in relazione alla mobilità quaternaria (Italian)- The evolution of the hydrographic network in the central Piedmont related to the Quaternary mobility. In: Polino, R., Sacchi, R. (Eds.), *Rapporti Alpi-Appennino Accad. Naz. Scienze*, (14), 445-461, 1995

725 Cassardo, C., Cremonini, R., Gandini, D., Paesano, G., Pelosini, R. and Qian, M.W.: Analysis of the severe flood of 13-16th October 2000 in Piedmont (Italy). *Cuadernos de Investigación Geográfica*, 27, pp.147-162., DOI: <http://dx.doi.org/10.18172/cig.1120>, 2013.

Clement, M.A., Kilsby, C.G. and Moore, P.: Multi-Temporal SAR Flood Mapping using Change Detection, *Journal of Flood Risk Management*, doi: <https://doi.org/10.1111/jfr3.12303>, 2017.

730 Copernicus Emergency Management Service (© 2016 European Union), EMSR192 - Floods in Northern Italy, available at <http://emergency.copernicus.eu/mapping/list-of-components/EMSR192>, 2016-(accessed 01/12/17/07/17) 2016.

Copernicus Emergency Management Service (© 2016 European Union), [EMSR192] Moncalieri: Grading Map available at <http://emergency.copernicus.eu/mapping/list-of-components/EMSR192>

Formattato: Inglese (Regno Unito)

Formattato: Inglese (Regno Unito)

Formattato: Inglese (Regno Unito)

~~components/EMSR192/ALL/EMSR192_18MONCALIERI~~http://emergency.copernicus.eu/mapping/list-of-components/EMSR192/ALL/EMSR192_18MONCALIERI (accessed 01/12/17), 2016

Costabile, P., Macchione, F., Natale, L. and Petaccia, G.: Flood mapping using LIDAR DEM. Limitations of the 1-D modeling highlighted by the 2-D approach, *Nat. Hazards*, 77(1), 181-204, doi: <https://doi.org/10.1007/s11069-015-1606-0>, 2015.

~~Clement, M.A., Kilsby, C.G. and Moore, P.: Multi-Temporal SAR Flood Mapping using Change Detection, *Journal of Flood Risk Management*, doi: <https://doi.org/10.1111/jfr3.12303>, 2017.~~

De Moel, H., Van Alphen, J., and Aerts, J. C. J. H.: Flood maps in Europe – methods, availability and use, *Nat. Hazards Earth Syst. Sci.*, 9, 289-301, <https://doi.org/10.5194/nhess-9-289-2009>, 2009.

De Zan, F. and Monti-Guarnieri, A., 2006. TOPSAR: Terrain observation by progressive scans. *IEEE Transactions on Geoscience and Remote Sensing*, 44(9), pp.2352-2360.

Farfaglia, S., Lollino, G., Iaquina, M., Sale, I., Catella, P., Martino, M. and Chiesa, S.: The use of UAV to monitor and manage the territory: perspectives from the SMAT project. In *Engineering Geology for Society and Territory-Volume 5* (pp. 691-695). Springer, Cham, https://doi.org/10.1007/978-3-319-09048-1_134, 2015

Fayne, J., Bolten, J., Lakshmi, V. and Ahamed, A.: Optical and Physical Methods for Mapping Flooding with Satellite Imagery. In *Remote Sensing of Hydrological Extremes* (pp. 83-103). Springer International Publishing. doi: https://doi.org/10.1007/978-3-319-43744-6_6, 2017.

Feng, Q., Liu, J. and Gong, J.: Urban flood mapping based on unmanned aerial vehicle remote sensing and random forest classifier—A case of Yuyao, China, *Water*, 7(4), 1437-1455, doi: <https://doi.org/10.3390/w7041437>, 2015.

Fiorucci, F., Giordan, D., Santangelo, M., Dutto, F., Rossi, M., and Guzzetti, F.: Criteria for the optimal selection of remote sensing images to map event landslides, *Nat. Hazards Earth Syst. Sci. Discuss.*, <https://doi.org/10.5194/nhess-2017-111>, in review, 2017.

Fohringer, J., Dransch, D., Kreibich, H. and Schröter, K.: Social media as an information source for rapid flood inundation mapping, *Nat. Hazard Earth Sys*, 15(12), 2725-2738, doi: <https://doi.org/10.5194/nhess-15-2725-2015>, 2015.

~~Kreibich, H., Piroth, K., Seifert, I., Maiwald, H., Kunert, U., Schwarz, J., Merz, B. and Thieken, A.H.: Is flow velocity a significant parameter in flood damage modelling?, *Nat. Hazards Earth Syst. Sci.*, 9, 1679-1692, <https://doi.org/10.5194/nhess-9-1679-2009>, 2009.~~

- 760 Gao, B.C.: NDWI—A normalized difference water index for remote sensing of vegetation liquid water from space, *Remote sensing of environment*, 58(3), 257-266, doi: [https://doi.org/10.1016/S0034-4257\(96\)00067-3](https://doi.org/10.1016/S0034-4257(96)00067-3), 1996.
- Gianinetto, M., Villa, P. and Lechi, G.: Postflood damage evaluation using Landsat TM and ETM+ data integrated with DEM, *IEEE Transactions on Geoscience and Remote Sensing*, 44(1), 236-243, doi: <https://doi.org/10.1109/TGRS.2005.859952>, 2006.
- 765 Giordan, D., Manconi, A., Facello, A., Baldo, M., Allasia, P. and Dutto, F.: Brief Communication: The use of an unmanned aerial vehicle in a rockfall emergency scenario. ~~*Natural, Nat. Hazards and Earth System Sciences, Syst. Sci.*~~, 15(1), pp.163-169, doi: <https://doi.org/10.5194/nhess-15-163-2015>, 2015.
- Giordan D., Manconi A., Remondino F. and Nex F.: Use of unmanned aerial vehicles in monitoring application and management of natural hazards, *Geomatics, Natural Hazards and Risk*, 8:1, 1-4, DOI: <https://doi.org/10.1080/19475705.2017.1315619>, 2017.
- 770 Giustarini, L., Hostache, R., Matgen, P., Schumann, G. J. P., Bates, P. D., & and Mason, D. C.: A change detection approach to flood mapping in urban areas using TerraSAR-X, *IEEE transactions on Geoscience and Remote Sensing*, 51(4), 2417-2430. doi: [0.1109/TGRS.2012.2210901](https://doi.org/10.1109/TGRS.2012.2210901), 2013.
- Griesbaum, L., Marx, S. and Höfle, B.: Direct local building inundation depth determination in 3-D point clouds generated from user-generated flood images. *Natural Hazards and Earth System Sciences*, 17(7), p.1191, 2017.
- 775 ~~Guy J. P., Schumann, Delwyn K., Moller, Microwave remote sensing of flood inundation, *Physics and Chemistry of the Earth, Parts A/B/C, Volume 83, Pages 84-95, ISSN 1474-7065, http://dx.doi.org/10.1016/j.pce.2015.05.002*, 2015.~~
- Hung, K.C., Kalantari, M. and Rajabifard, A.: Methods for assessing the credibility of volunteered geographic information in flood response: A case study in Brisbane, Australia, *Applied Geography*, 68, 37-47, doi: <https://doi.org/10.1016/j.apgeog.2016.01.005>, 2016.
- 780 [Ireland, G., Volpi, M. and Petropoulos, G.P.: Examining the capability of supervised machine learning classifiers in extracting flooded areas from Landsat TM imagery: A case study from a Mediterranean flood. *Remote Sensing*, 7\(3\), 3372-3399. doi: https://doi.org/10.3390/rs70303372, 2015.](https://doi.org/10.3390/rs70303372)
- ~~Justice, C.O., Vermote, E., Townshend, J.R., Defries, R., Roy, D.P., Hall, D.K., Salomonson, V.V., Privette, J.L., Riggs, G., Strahler, A. and Lucht, W. Justice, C.O., Vermote, E., Townshend, J.R., Defries, R., Roy, D.P., Hall, D.K., Salomonson, V.V.,~~
- 785

Privette, J.L., Riggs, G., Strahler, A. and Lucht, W.: The Moderate Resolution Imaging Spectroradiometer (MODIS): Land remote sensing for global change research, IEEE Transactions on Geoscience and Remote Sensing, 36(4), 1228-1249, 1998.

Kreibich, H., Piroth, K., Seifert, I., Maiwald, H., Kunert, U., Schwarz, J., Merz, B. and Thieken, A.H.: Is flow velocity a significant parameter in flood damage modelling?. Nat. Hazards Earth Syst. Sci., 9, 1679-1692, <https://doi.org/10.5194/nhess-9-1679-2009>, 2009.

Luino, F., Cirio, C.G., Biddoccu, M., Agangi, A., Giulietto, W., Godone, F. and Nigrelli, G.: Application of a model to the evaluation of flood damage, Geoinformatica, 13(3), 339-353, doi: 10.1007/s10707-008-0070-3, 2009.

Luino, F.: The flood and landslide event of November 4–6 1994 in Piedmont Region (Northwestern Italy): Causes and related effects in Tanaro Valley, Physics and Chemistry of the Earth, Part A: Solid Earth and Geodesy, 24(2), 123-129, doi: [https://doi.org/10.1016/S1464-1895\(99\)00007-1](https://doi.org/10.1016/S1464-1895(99)00007-1), 1999.

Ireland, G., Volpi, M. and Petropoulos, G.P.: Examining the capability of supervised machine learning classifiers in extracting flooded areas from Landsat TM imagery: A case study from a Mediterranean flood, Remote Sensing, 7(3), 3372-3399, doi: <https://doi.org/10.3390/rs70303372>, 2015.

Mason D.C., Giustarini L., Garcia-Pintado J., Cloke H.L.: Detection of flooded urban areas in high resolution Synthetic Aperture Radar images using double scattering, International Journal of Applied Earth Observation and Geoinformation, Volume 28, Pages 150-159, ISSN 0303-2434, <http://dx.doi.org/10.1016/j.jag.2013.12.002>, 2014.

Meesuk, V., Vojinovic, Z., Mynett, A.E. and Abdullah, A.F.: Urban flood modelling combining top-view LiDAR data with ground-view SfM observations, Advances in Water Resources, 75, 105-117, doi: <https://doi.org/10.1016/j.advwatres.2014.11.008>, 2015.

Merz, B., Kreibich, H., Schwarze, R., and Thieken, A.: Review article "Assessment of economic flood damage", Nat. Hazards Earth Syst. Sci., 10, 1697-1724, <https://doi.org/10.5194/nhess-10-1697-2010>, 2010.

Nigro, J., Slayback, D., Policelli, F. and Brakenridge, G.R.: NASA/DFO MODIS near real-time (NRT) global flood mapping product evaluation of flood and permanent water detection. Evaluation, Greenbelt, MD, 2014.

Paprotny, D., Morales-Nápoles, O., and Jonkman, S. N.: Efficient pan-European river flood hazard modelling through a combination of statistical and physical models, Nat. Hazards Earth Syst. Sci., 17, 1267-1283, <https://doi.org/10.5194/nhess-17-1267-2017>, 2017.

Pulvirenti, L., Chini, M., Pierdicca, N., Guerriero, L. and Ferrazzoli, P.: Flood monitoring using multi-temporal COSMO-SkyMed data: Image segmentation and signature interpretation, *Remote Sensing of Environment*, 115(4),990-1002, doi: <https://doi.org/10.1016/j.rse.2010.12.002>, 2011.

815 Perks, M. T., Russell, A. J., and Large, A. R. G.: Technical Note: Advances in flash flood monitoring using unmanned aerial vehicles (UAVs), *Hydrol. Earth Syst. Sci.*, 20, 4005-4015, <https://doi.org/10.5194/hess-20-4005-2016>, 2016.

Pierdicca, N., Pulvirenti, L. and Chini, M.: Flood Mapping in Vegetated and Urban Areas and Other Challenges: Models and Methods. In Flood Monitoring through Remote Sensing (pp. 135-179). Springer, Cham., https://doi.org/10.1007/978-3-319-63959-8_7, 2018

820 Pinto, J.G., Ulbrich, S., Parodi, A., Rudari, R., Boni, G. and Ulbrich, U.: Identification and ranking of extraordinary rainfall events over Northwest Italy: The role of Atlantic moisture, *Journal of Geophysical Research: Atmospheres*, 118(5), 2085-2097, doi: <https://doi.org/10.1002/jgrd.50179>, 2013.

Pulvirenti, L., Chini, M., Pierdicca, N., Guerriero, L. and Ferrazzoli, P.: Flood monitoring using multi-temporal COSMO-SkyMed data: Image segmentation and signature interpretation. *Remote Sensing of Environment*, 115(4),990-1002. doi: <https://doi.org/10.1016/j.rse.2010.12.002>, 2011.

825 Rahman, M.S. and Di, L.: The state of the art of spaceborne remote sensing in flood management, *Natural Hazards*, 85(2), 1223-1248., doi: <https://doi.org/10.1007/s11069-016-2601-9>, 2017.

Refice, A., Capolongo, D., Pasquariello, G., D'Addabbo, A., Bovenga, F., Nutricato, R., Lovergine, F.P. and Pietranera, L.: SAR and InSAR for flood monitoring: Examples with COSMO-SkyMed data, *IEEE Journal of Selected Topics in Applied Earth Observations and Remote Sensing*, 7(7), 2711-2722, doi: <https://doi.org/10.1109/JSTARS.2014.2305165>, 2014.

830 Regione Piemonte: Gli eventi alluvionali del settembre-ottobre 1993 in Piemonte (Italian), <http://www.arpa.piemonte.gov.it/approfondimenti/temi-ambientali/geologia-e-dissesto/pubblicazioni/immagini-e-files/ev93>, (accessed 01/12/17), 1996.

Rosser, J.F., Leibovici, D.G. and Jackson, M.J.: Rapid flood inundation mapping using social media, remote sensing and topographic data, *Natural Hazards*, 87(1), 103-120, doi: <https://doi.org/10.1007/s11069-017-2755-0>, 2017.

Segura-Beltrán, F., Sanchis-Ibor, C., Morales-Hernández, M., González-Sanchis, M., Bussi, G. and Ortiz, E.: Using post-flood surveys and geomorphologic mapping to evaluate hydrological and hydraulic models: The flash flood of the Girona River (Spain) in 2007, *Journal of Hydrology*, 541, pp.310-329. <https://doi.org/10.1016/j.jhydrol.2016.04.039>, 2016.

Formattato: Testo commento, Interlinea: 1.5 righe

Formattato: Tipo di carattere: Times New Roman, Colore carattere: Nero, Non Evidenziato

840 ~~Smith, M. W., J. L. Carriviek, J. Hooke, and Kirkby M. J.: Reconstructing flash flood magnitudes using ‘Structure-from-Motion’: A rapid assessment tool, Journal of Hydrology 519, pp 1914-1927, doi: <https://doi.org/10.1016/j.jhydrol.2014.09.078>, 2014.~~

Schnebele, E. and Cervone, G.: Improving remote sensing flood assessment using volunteered geographical data, Nat. Hazards Earth Syst. Sci., 13, 669-677, <https://doi.org/10.5194/nhess-13-669-2013>, 2013.

845 Shrestha, R., Di, L., Eugene, G.Y., Kang, L., SHAO, Y.Z. and BAI, Y.Q.: Regression model to estimate flood impact on corn yield using MODIS NDVI and USDA cropland data layer-, Journal of Integrative Agriculture, 16(2), 398-407, doi: [https://doi.org/10.1016/S2095-3119\(16\)61502-2](https://doi.org/10.1016/S2095-3119(16)61502-2), 2017.

~~Smith, M. W., J. L. Carriviek, J. Hooke, and Kirkby M. J.: Reconstructing flash flood magnitudes using ‘Structure-from-Motion’: A rapid assessment tool, Journal of Hydrology 519, pp 1914-1927, doi: <https://doi.org/10.1016/j.jhydrol.2014.09.078>, 2014.~~

850 Schumann, G.J.P. and Moller, D.K.: Microwave remote sensing of flood inundation. Physics and Chemistry of the Earth, Parts A/B/C, 83, pp.84-95., doi: <https://doi.org/10.1016/j.pce.2015.05.002>, 2015

Snavely, N., Seitz, S.M. and Szeliski, R.: Modelling the world from internet photo collections, International Journal of Computer Vision, 80(2), 189-210, doi: <https://doi.org/10.1007/s11263-007-0107-3>, 2008.

855 Tapia-Silva, F.O., Itzerott, S., Foerster, S., Kuhlmann, B. and Kreibich, H.: Estimation of flood losses to agricultural crops using remote sensing, Physics and Chemistry of the Earth, Parts A/B/C, 36(7), 253-265, doi: <https://doi.org/10.1016/j.pce.2011.03.005>, 2011.

Torres, R., Snoeij, P., Geudtner, D., Bibby, D., Davidson, M., Attema, E., Potin, P., Rommen, B., Floury, N., Brown, M. and Traver, I.N.: GMES Sentinel-1 mission-, Remote Sensing of Environment, 120, pp.9-24-, doi: <https://doi.org/10.1016/j.rse.2011.05.028>, 2012.

860 -Vermote E. - NASA GSFC and MODAPS SIPS – NASA: MYD09 MODIS/Aqua L2 Surface Reflectance, 5-Min Swath 250m, 500m, and 1km. NASA LP DAAC, doi: <http://doi.org/10.5067/MODIS/MYD09.006>, 2015

Yan, K., Di Baldassarre, G., Solomatine, D.P. and Schumann, G.J.P.: A review of low-cost space-borne data for flood modelling: topography, flood extent and water level-, Hydrological Processes, 29(15), 3368-3387, doi: <https://doi.org/10.1002/hyp.10449>, 2015.

865 Wang, Y., Colby, J.D. and Mulcahy, K.A.: An efficient method for mapping flood extent in a coastal floodplain using Landsat
 TM and DEM data, International Journal of Remote Sensing, 23(18), 3681-3696, doi:
<https://doi.org/10.1080/01431160110114484>, 2012.

Westoby, M. J., J. Brasington, N. F. Glasser, M. J. Hambrey, and Reynolds J.M.: 'Structure-from-
 Motion' photogrammetry: A low-cost, effective tool for geoscience applications, Geomorphology
 179, 300-314, doi: <https://doi.org/j.geomorph.2012.08.02>, 2012.

Xu, H.: Modification of normalised difference water index (NDWI) to enhance open water features in remotely sensed
 imagery, International journal of remote sensing, 27(14), 3025-3033, doi: <https://doi.org/10.1080/01431160600589179>, 2006.

Zhang, D. and Zhou, G.: Estimation of Soil Moisture from Optical and Thermal Remote Sensing: A Review, Sensors, 16(8),
 p.1308, doi: <https://doi.org/1016/j.pce.2011.03.005>, 2016.

875

880

Table 1. Resume of ~~dataset~~the datasets used to map and characterize flooded area in this study

| Type | Sensor used | Spatial resolution (m) | Covered area by single scene (km ²) | Min. Revisit time (Day) |
|--------------------------------|---------------|------------------------------------|---|----------------------------|
| 1 – Satellite Data | | | | |
| SAR –X band | Cosmo-SkyMed | 60 | > 1'000 | 4 |
| SAR- C band | Sentinel-1A/B | 5 (ground range) x 20 (azimuth) | > 10'000 | 6 |
| Multi-spectral | MODIS-Aqua | 500 | > 100'0000 | Daily |
| Multi-spectral | Sentinel-2 | 10 / 20 | > 10'000 | 10 (5) |
| 2- Aerial data | | | | |
| Very High res. visible band | Tecnam P92-JS | 0.01 | 100 km ² | On-demand |

| | | | | |
|------------------------------------|---------------------------------|-------------|----------------------|--------------|
| Ultra-High resolution visible band | RPASs CarbonCore 950 octocopter | 0.02 / 0.03 | < 10 km ² | On-demand |
| DTM LIDAR | Airborne | 5 | Piemonte region | Archive data |
| 3- Ground-Based | | | | |
| Photo / video from car platform | GO-PRO HERO 3+ | 0.02 / 0.03 | Local /urban | On demand |

885

Table 2. Resume of satellite data in relation with flood stage

| Satellite | Spatial Resolution | Acquisition time | | |
|----------------|--------------------|------------------------|------------------------|------------|
| | | Pre-flood | Co-flood | Post-flood |
| Cosmo-SkyMed | Medium | 05:05 UTC – 25/11/2016 | | |
| Sentinel-1 A/B | Medium | 05:35 UTC – 22/11/2016 | 05:35 UTC – 28/11/2016 | |
| MODIS Aqua | Medium-Low | 12:30 UTC - 12/11/2016 | 12:30 UTC - 26/11/2016 | |
| Sentinel-2 | Medium-High | 15:19 UTC - 11/11/2016 | 14:19 UTC – 01/12/2016 | |

890

Table 3. Characteristics of the Sentinel-1 dataset used in this study

| | |
|---------------------------|---------------------------|
| Satellite | Sentinel-1 A/B |
| Sensor Parameter | C-band 5.405 GHz |
| Orbit | Descending |
| Pre-flood acquisitions | 22/11/2016 |
| Post-flood acquisitions | 28/11/2016 |
| Data format | Single Look Complex (SLC) |
| Azimuth pixel spacing [m] | ~13 |
| Range pixel spacing [m] | ~2 |

895

Table 4. Characteristics of the Aqua MODIS data used in this work.

| Band | Bandwidth nm | Band type | Spatial resolution (m) |
|------|--------------|-----------|------------------------|
| B1 | 620 – 670 | Red | 500 |
| B2 | 841 – 876 | NIR | 500 |
| B3 | 459 – 479 | Blue | 500 |
| B4 | 545 – 565 | Green | 500 |
| B5 | 1230 – 1250 | SWIR | 500 |
| B7 | 2105 – 2155 | SWIR | 500 |

Table 5. Characteristics of Sentinel-2 data used in this work.

| Band | Wavelength nm | Band type | Spatial resolution (m) |
|------|---------------|-----------|------------------------|
| B2 | 490 | Blue | 10 |
| B3 | 560 | Green | 10 |
| B4 | 665 | Red | 10 |
| B8 | 842 | NIR | 10 |
| B5 | 705 | NIR | 20 |
| B6 | 740 | NIR | 20 |
| B7 | 783 | NIR | 20 |
| B8a | 865 | NIR | 20 |
| B11 | 1610 | SWIR | 20 |
| B12 | 2190 | SWIR | 20 |

Table 6. Accuracy in automatic flooded and not flooded area detection

| Sector | Area km ² | Sentinel-2 | | MODIS-Aqua | | | CSKM | Sentinel-1 |
|-----------------|----------------------|----------------------|---------------------|----------------------|-----|-----|-----------|------------------|
| | | MNDWI _{var} | NDVI _{var} | MNDWI _{var} | MLC | SA | Recl Ampl | $\Delta\sigma^0$ |
| Not Flooded | 259.5 | 87% | 87% | 91% | 94% | 95% | 96% | 99% |
| Flooded area | | | | | | | | |
| - Po | 47.8 | 48% | 37% | 49% | 70% | 64% | 23% | 4% |
| - Oitana | 11.6 | 49% | 42% | 60% | 11% | 36% | 37% | 1% |
| - Chisola | 7.3 | 21% | 51% | 30% | 24% | 23% | 12% | 1% |
| - Chisola urban | 1.1 | 4% | 24% | | | | | |

Commentato [ND10]: This table added according to the RC -11 of reviewer 1

Table 7. Water height measures obtained from structure from motion, GPS survey and simulation with DTM

| Measure point coordinates | | Water Depth (m) | | |
|---------------------------|---------|-----------------|------|---------------|
| UTM X | UTM Y | SfM (+/- 0.05) | GPS | DTM (+/- 0.2) |
| 395132 | 4983240 | 1.56 | 1.60 | 1.61 |
| 395242 | 4983152 | 1.45 | 1.40 | 1.42 |
| 395140 | 4982644 | 0.84 | 0.78 | 1.01 |
| 395142 | 4981624 | 0.82 | 0.81 | 0.78 |
| 395022 | 4981188 | 1.28 | 1.35 | 1.56 |
| 394877 | 4980993 | 1.40 | 1.37 | 1.34 |

905

910

915

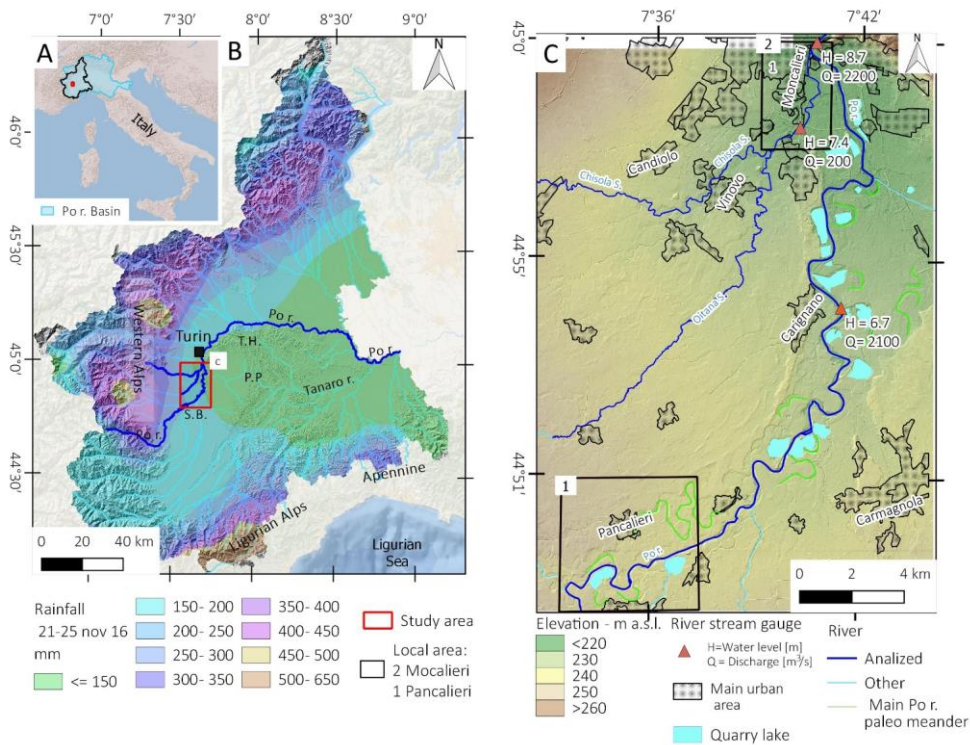
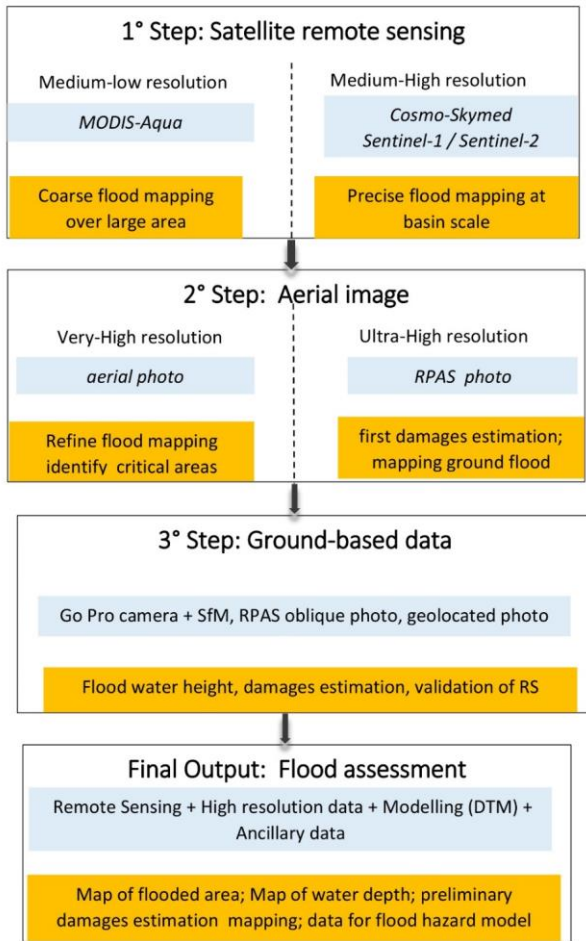
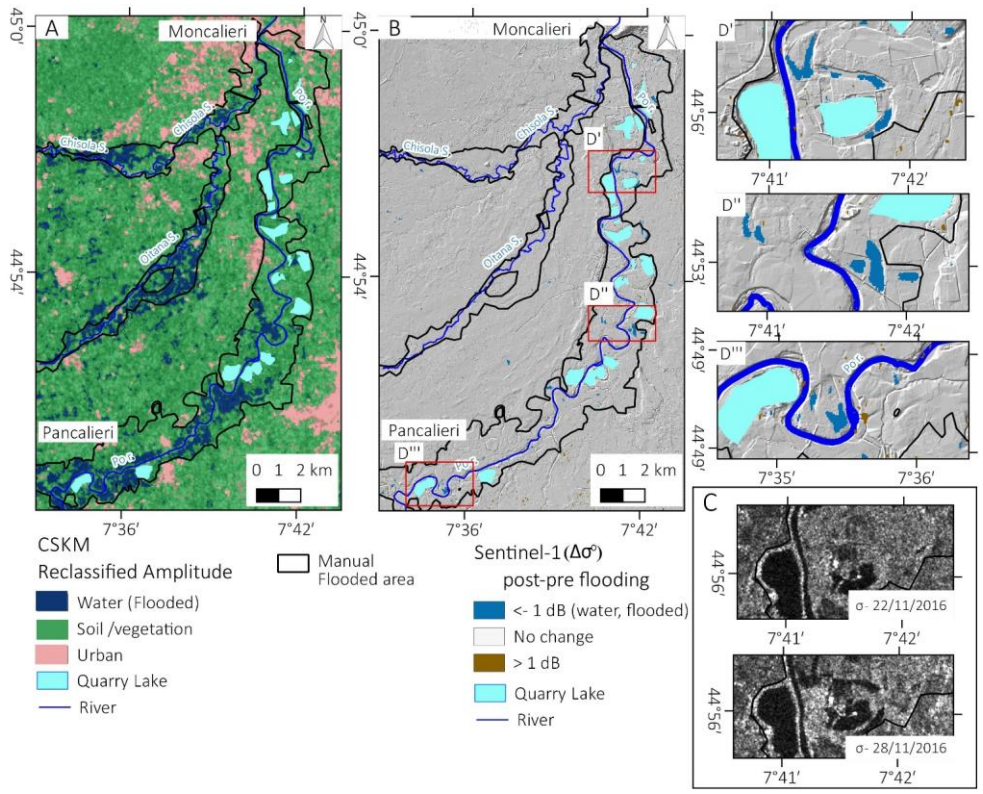


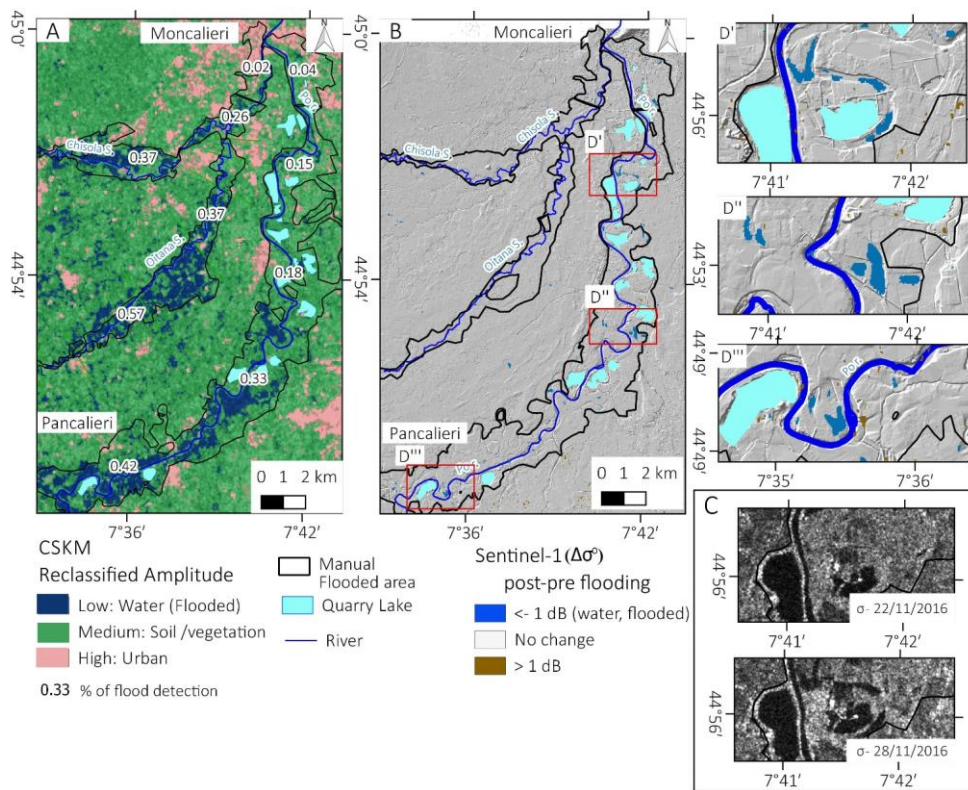
Figure 1: A) Location of Piemonte region in Italy, **B)** Rainfall in Piemonte region during the 21-25 November flood event (Based on ARPA Piemonte data) and location of study area, S. B. = Savigliano Basin, P. P. = Poirino Plateau, T.H = Turin Hills; C) Detailed view of the study area with discharge in the stream gauge stations and the location of Pancalieri (1) and Moncalieri (2) local areas case [Historyhistory](#).



Formattato: Giustificato

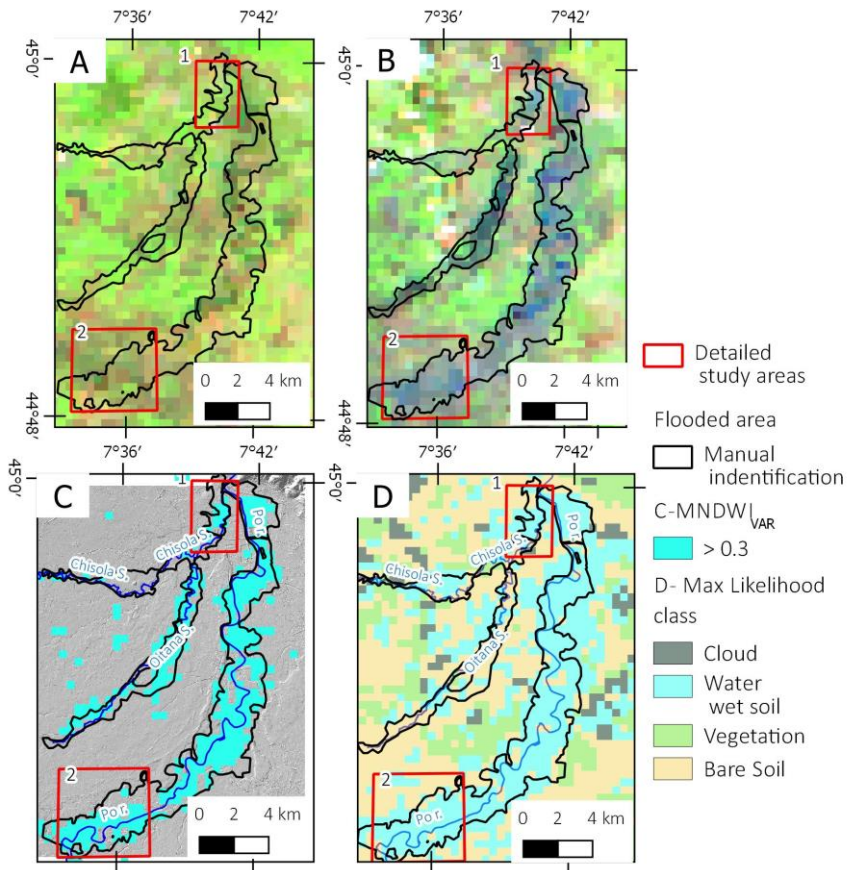
Figure 2: The flowchart illustrating the multiscale flood mapping approaches proposed in this work





930 **Figure 3: A) Reclassified Quicklook Amplitude SAR Image acquired at 05:05 UTC of 25 November 2016 - COSMO-SkyMed© ASI [2016] - B) Sentinel-1 geocoded backscattering coefficient difference ($\Delta\sigma$); C) Example of change backscattering between the pre- and the post-flood image is clearly detectable. D'; D'' D''') detail of some areas where Sentinel-1 $\Delta\sigma$ still detect water.**

Formattato: Tipo di carattere: Non Grassetto



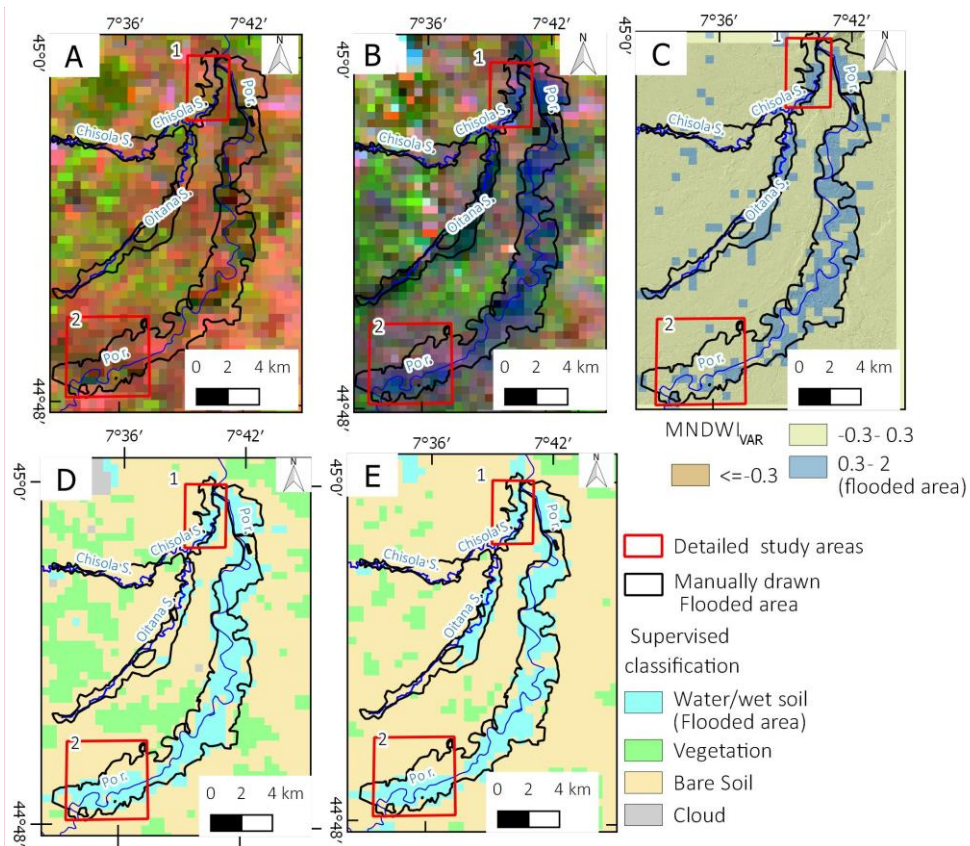


Figure 4: MODIS Aqua satellite image A) False colour band composition 7-2-1 acquired the 12 November 2016.; B) False colour band composition 7-2-1 acquired the 26 November 2016.; C) automatic detection of the flooded area using $MNDWI_{var} >>> 0.3$; D) automatic detection of the flooded area using supervised classification with maximum likelihood classification method (D) and with spectral angle method (E). The red box identifies the local case history of Moncaleri (1) and Pancalieri (2)

Formattato: Giustificato

Commentato [ND11]: Image modified according to RC-7 of reviewer 1

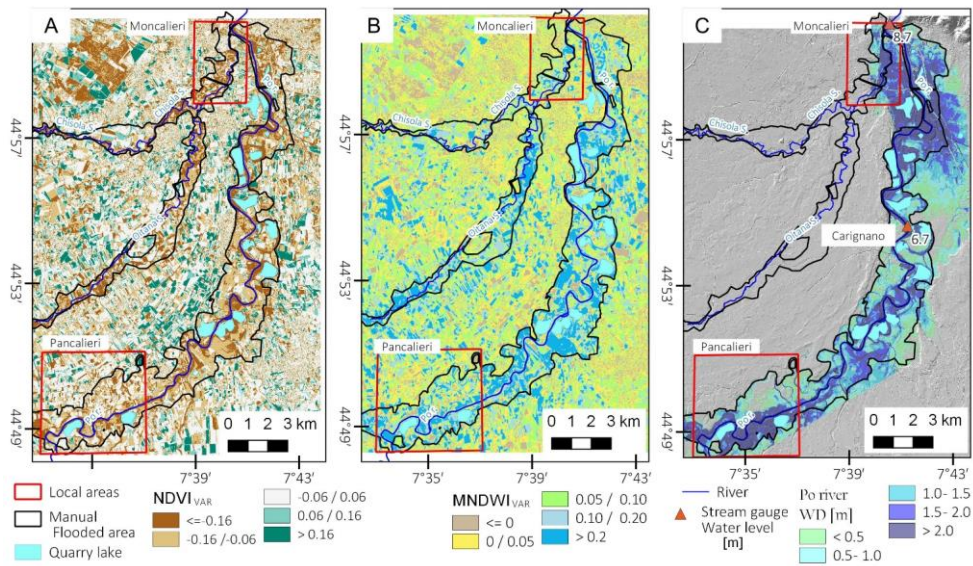


Figure 5: Sentinel-2 analysis and validation: A) NDVI variation 10 m of spatial resolution, B) MNDWI variation 20 m of spatial resolution, C) Simulation of flooded area water depth for Po river based on 5-m DTM and river height level registered in Arpa Piemonte stream gauge.

940

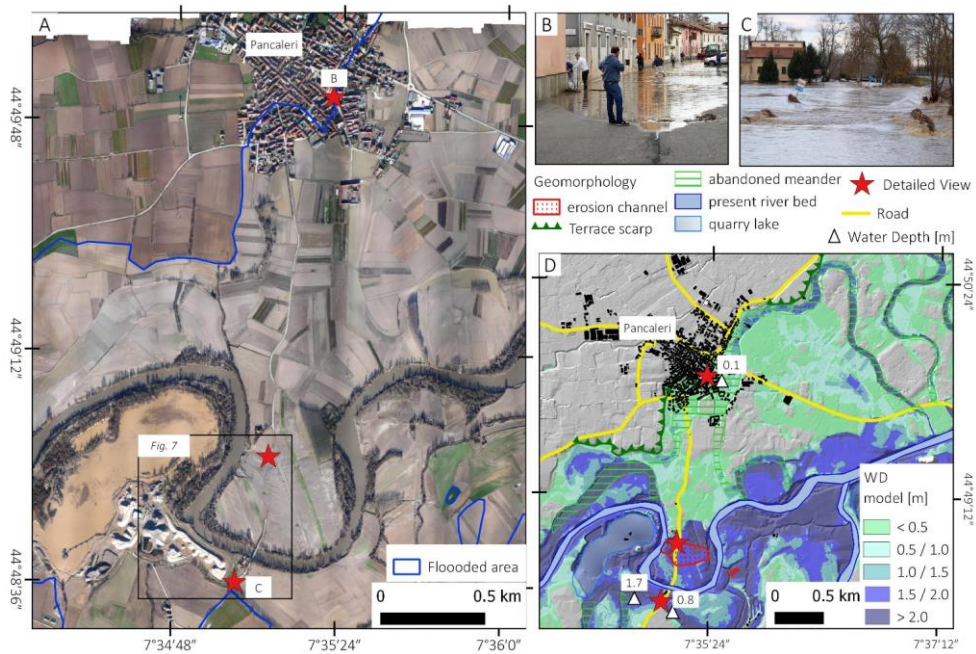


Figure 6: A) Aerial photo at 10 cm of resolution taken the 28 November 2016; B and C) photo took from a local newspaper and geolocalized with Google Streetview; D) Geomorphological elements and model of estimated water depth (m).

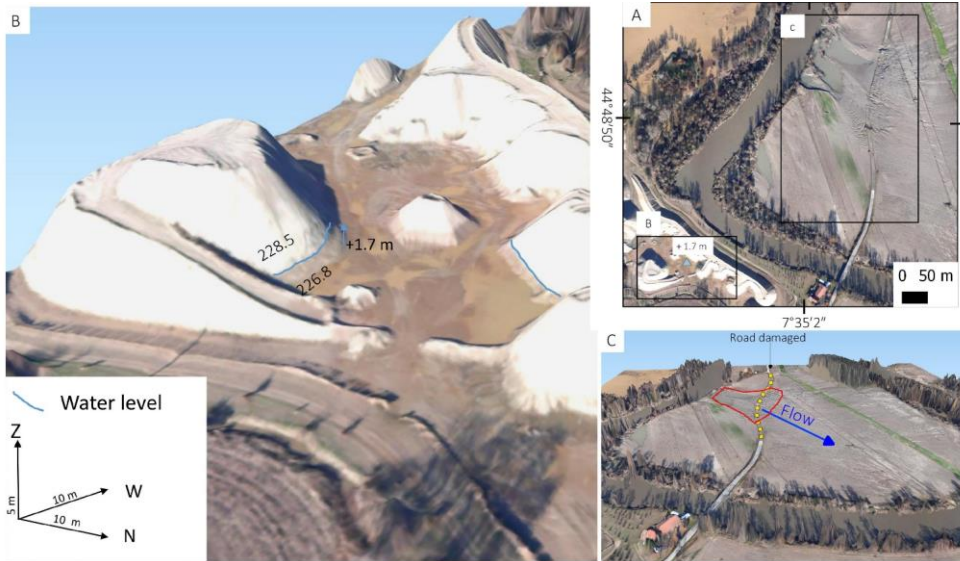


Figure 7: The SfM 3-D model obtained from very high-resolution aerial photo, near Po River at the south of Pancalieri (A) allowed to measure: B) Measuring the approximate height-on-water depth on a sand deposits of a quarry (B) near Po River at south of Pancalieri (A) and to observe A); C) Mapping the effect of meander cut a: an erosion channel and the destruction along a stretch of road (C).

950

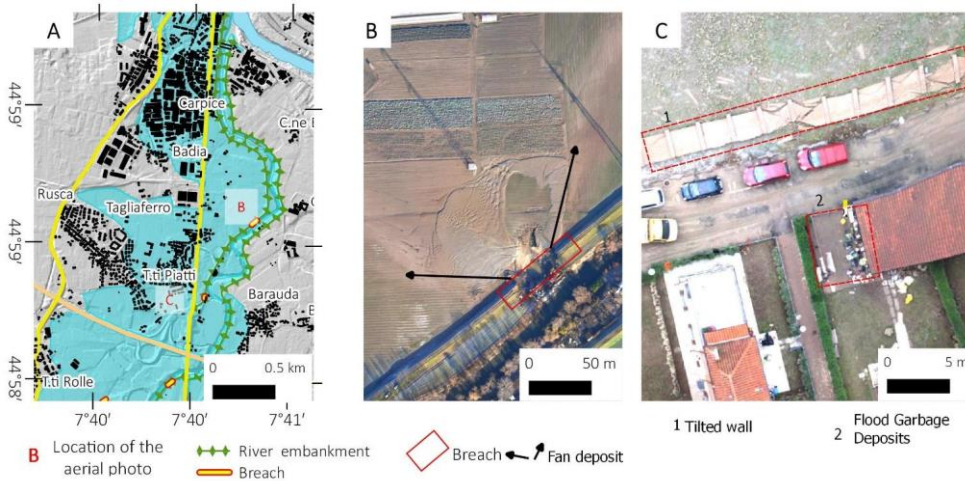
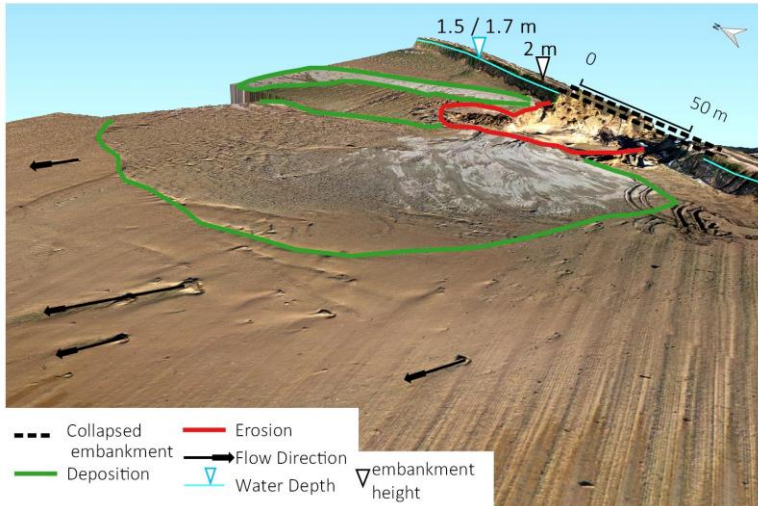


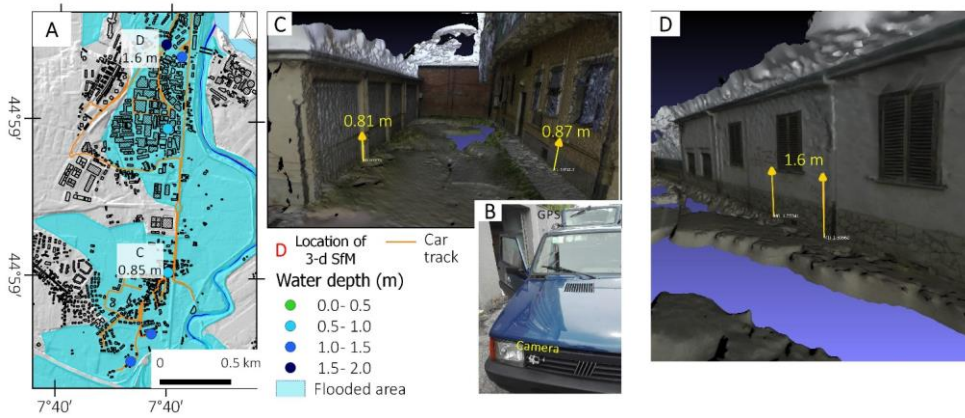
Figure 8: A) map of flooded Chisola flooded area in Moncalieri municipality with location of detailed photo; B) Aerial photo at 0.1 m of resolution showing the breach of river embankment and the ‘alluvial fan’ created by water flow showed with a 3-d view in figure 9; C) RPASs photo at 0.02 m of spatial resolution showing a collapsed wall in the Tetti Piatti area and the deposit of damaged good from the nearby house.

Formattato: Giustificato



960

Figure 9: 3-D Model derived from the RPASs aerial photo and SfM elaborations photo overlap. The model shows the river embankment rupture (point B in figure 8A), -the geomorphological effects in the neighbour areas ~~and allowed the estimation of. It is also possible to estimate~~ water depth from the signs on the embankment.



965 Figure 10: A) Map of the flooded area by Chisola stream in the Moncalieri municipality with measured water height and location of 3-d photo; B) Installation of the GO-PRO HERO 3+ (Black Edition) camera and GPS antenna over the car (the processing system for STANAG 4609 encoding was installed inside the car); C and D) Examples 3-d models made with Structure from Motion in which was possible to measure the water height. ↴

Formattato: Giustificato

Formattato: Tipo di carattere: 9 pt, Grassetto

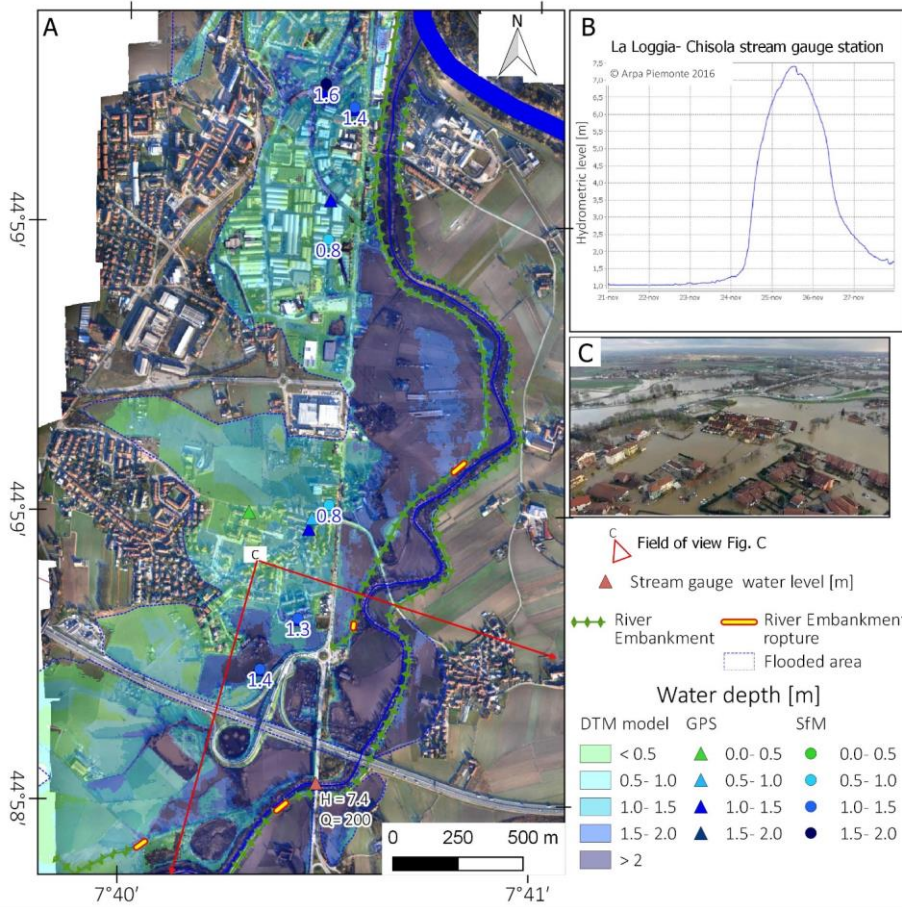
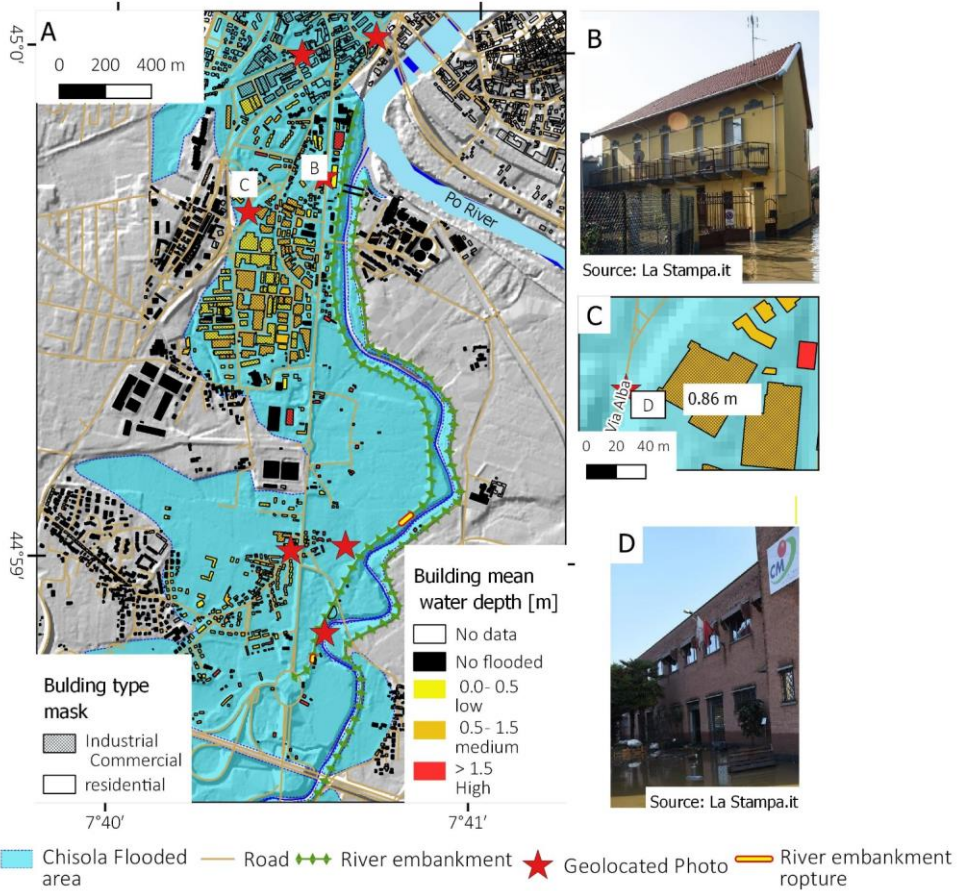


Figure 11: A) Water depth levee map based on SfM data and 5-m DTM model; B) Water level reached by Chisola stream in ARPA Piemonte station; C) Geolocated third part photo: 25/11/2016 aerial view of flooded area find on the web (<https://vivere-moncalieri.it/2016/11/30/3760/>)



975 **Figure 12:** A) Water level height map based on SfM data and 5-m DTM model; C) Zoom on the building of figure D; B and D) Photo where it is possible to observe the water depth from the newspaper “La Stampa” geolocated using Google Street view.

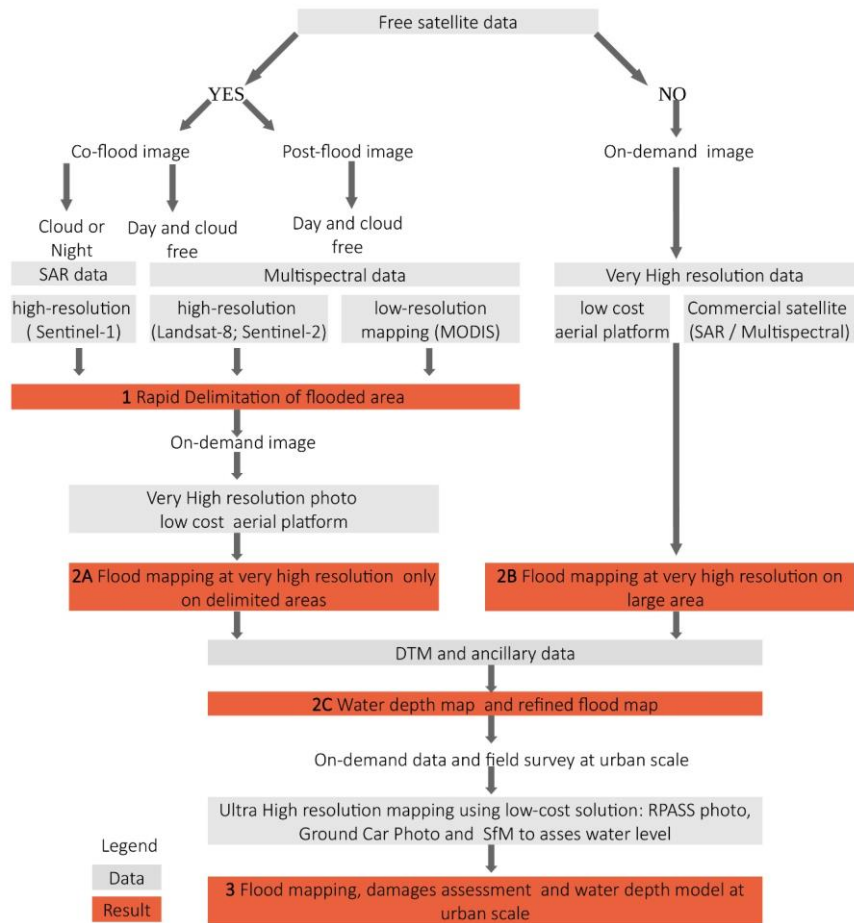


Figure 13: Flowchart of the proposed flood mapping strategy.

Formattato: Giustificato

Formattato: Tipo di carattere: 9 pt, Grassetto